AGU PUBLICATIONS

Tectonics

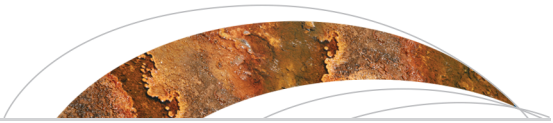

RESEARCH ARTICLE
10.1002/2014TC003803

Key Points:
- Yong'an Basin, southeast China was a retroarc foreland basin in Permian-Jurassic
- Accretionary orogenic belt developed along SE margin of SCC in Permian-Jurassic
- Both Paleo-Tethys and Paleo-Pacific affect the Permian-Triassic event in the SCC

Supporting Information:
- Supporting Information S1
- Dataset S1
- Dataset S2
- Dataset S3

Correspondence to:
Y. Du,
duyuansheng126@126.com

Citation:
Hu, L., P. A. Cawood, Y. Du, J. Yang, and L. Jiao (2015), Late Paleozoic to Early Mesozoic provenance record of Paleo-Pacific subduction beneath South China, *Tectonics*, *34*, 986–1008, doi:10.1002/2014TC003803.

Received 16 DEC 2014
Accepted 13 APR 2015
Accepted article online 16 APR 2015
Published online 22 MAY 2015

Late Paleozoic to Early Mesozoic provenance record of Paleo-Pacific subduction beneath South China

Lisha Hu[1,2], Peter A. Cawood[3,4], Yuansheng Du[1,2], Jianghai Yang[1,2], and Liangxuan Jiao[1,2]

[1]State Key Laboratory of Biogeology and Environmental Geology, China University of Geosciences, Wuhan, China, [2]Faculty of Earth Sciences, China University of Geosciences, Wuhan, China, [3]Department of Earth Sciences, University of St. Andrews, St. Andrews, UK, [4]Centre for Exploration Targeting, School of Earth and Environment, University of Western Australia, Crawley, Western Australia, Australia

Abstract Northeast trending Yong'an Basin, southeast South China Craton, preserves a Permian-Jurassic, marine to continental, siliciclastic-dominated, retroarc foreland basin succession. Modal and detrital zircon data, along with published paleocurrent data, sedimentary facies, and euhedral to subhedral detrital zircon shapes, indicate derivation from multicomponent, nearby sources with input from both the interior of the craton to the northwest and from an inferred arc accretionary complex to the southeast. The detrital zircon U-Pb age spectra range in age from Archean to early Mesozoic, with major age groups at 2000–1700 Ma, 1200–900 Ma, 400–340 Ma, and 300–240 Ma. In addition, Early Jurassic strata include zircon detritus with ages of 200–170 Ma. Regional geological relations suggest that Precambrian and Early Paleozoic detritus was derived from the inland Wuyi Mountain region and Yunkai Massif of the South China Craton. Sources for Middle Paleozoic to early Mesozoic detrital zircons include input from beyond the currently exposed China mainland. Paleogeographic reconstruction in East Asia suggests derivation from an active convergent plate margin along the southeastern rim of the craton that incorporated part of Southwest Japan and is related to the subduction of the Paleo-Pacific Ocean. Integration of the geologic and provenance records of the Yong'an Basin with the time equivalent Yongjiang and Shiwandashan basins that lie to the southwest and south, respectively, provides an integrated record of the subduction of the Paleo-Pacific Ocean along the southeast margin of the South China Craton and termination of subduction of the Paleo-Tethys beneath its southwest margin in Permo-Triassic.

1. Introduction

Asia consists of a series of crustal blocks that record a long history of continental amalgamation. A major pulse of amalgamation occurred in the Late Paleozoic to early Mesozoic as part of the final assembly of Eurasia. For example, the accretion of Indochina and South China along the Jinshajiang-Ailaoshan-Song Ma (Song Chay) zone [*Cai and Zhang*, 2009; *Faure et al*., 2014; *Lepvrier et al*., 2008, 1997; *Nakano et al*., 2008; *Zhao et al*., 2012], collision of the South China and North China cratons along the Qinling-Dabie Orogenic Belt [*Chang*, 1996; *Kim et al*., 2011; *Meng and Zhang*, 1999; *Zhang*, 1997], and the accretion of the Sibumasu Block to Indochina Block, as well as the accretion of numerous other smaller blocks [*Metcalfe*, 2002, 2006, 2011, 2013; *Wang et al*., 2013a]. In terms of paleogeographic reconstructions, this time period corresponds with the termination of subduction of the Paleo-Tethys beneath the southwestern margin of the South China Craton and the beginning of subduction of the Paleo-Pacific along the southeastern and eastern margin [e.g., *Cai and Zhang*, 2009; *Li et al*., 2012; *Li and Li*, 2007; *Zi et al*., 2012, 2013]. However, in detail the paleogeographic reconstructions are controversial. *Li and Li* [2007], also see *Li et al*. [2012], proposed that subduction of the Paleo-Pacific Ocean was initiated in early to middle Permian. Others have argued that during the Permo-Triassic the South China Craton was under the influence of the subduction and closure of the Paleo-Tethys Ocean and subsequent collisional tectonic activities between the South China Craton and Indochina Block [e.g., *Cai and Zhang*, 2009; *Shu et al*., 2008; *Yang et al*., 2012a, 2013], with subduction of the Paleo-Pacific not commencing until the Early to Middle Jurassic [e.g., *Zhou et al*., 2006]. These end-member models are not mutually exclusive, and subduction of both the Paleo-Tethys and Paleo-Pacific may have played a part in the evolution of South China, but in detail the interplay between the two has not been investigated and hence is an aim of this paper.

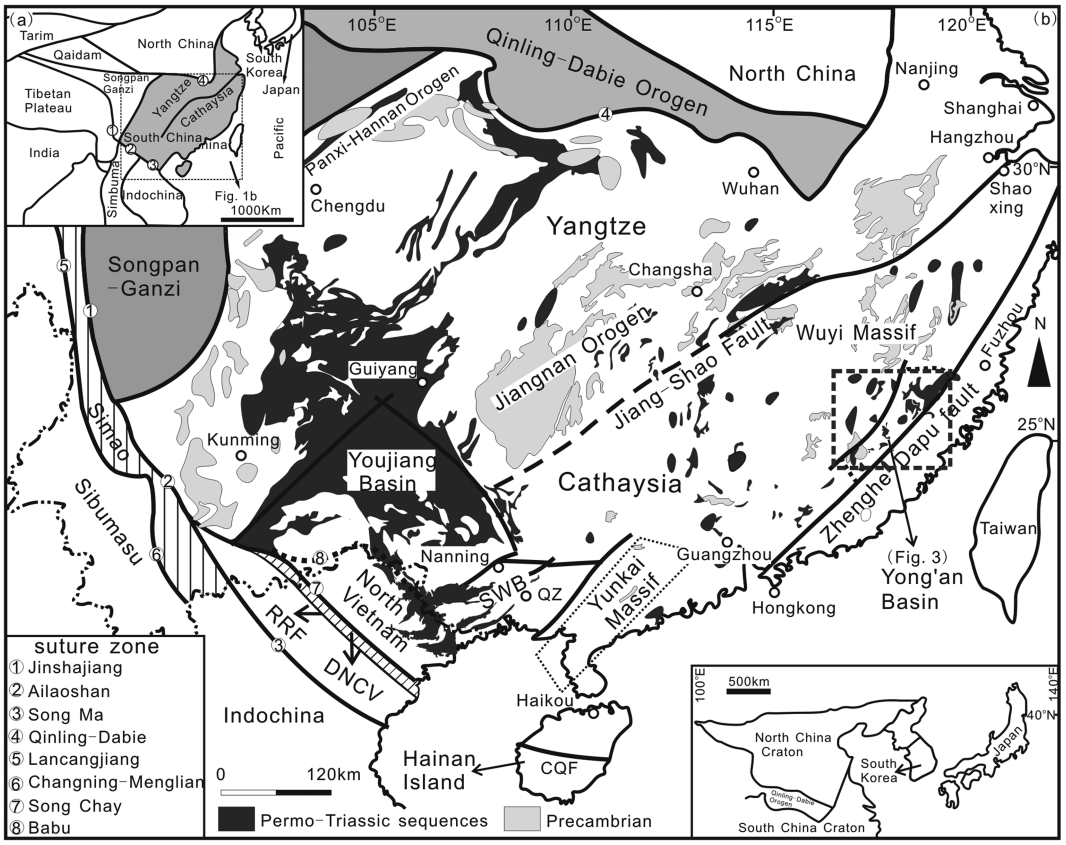

Figure 1. (a) Tectonic framework of the East Asia (modified from *Metcalfe* [2006]) and (b) simplified geological map of the South China Craton showing distribution of Precambrian and Permian-Triassic rock units in the southern of the Craton (based on the 1:5,000,000 geology map of China).

A number of studies have highlighted how sedimentology and detrital records of sedimentary basins can inform paleogeographic reconstructions by constraining the position, age, temporal and spatial trends, and tectonic setting of the sediment source [e.g., *Cawood*, 1983; *Cawood et al*., 2012, 2003; *Dickinson and Suczek*, 1979; *Sinclair*, 1997]. In this paper, we integrate petrologic modal, and detrital zircon U-Pb analyses of sandstones and siltstones from Middle Permian and Triassic to Early Jurassic strata in the Yong'an Basin, which is situated immediately inboard of the Pacific margin of the South China Craton. This data, in combination with data from time equivalent sequences to the southwest and west, along with regional constraints imposed by geological relations in Southwest Japan, indicate that the Yong'an Basin occupied a retroarc (back-arc) foreland basin setting related to the subduction of the Paleo-Pacific plate.

2. Geological Background

2.1. South China Craton

The Yong'an Basin, along with the Youjiang and Shiwandashan basins, formed a series of Late Paleozoic to Early Mesozoic depocenters along the southern margin of the South China Craton (Figure 1). The craton is bounded to the north by the Qinling-Dabie-Sulu Orogen [*Meng and Zhang*, 1999; *Zhang*, 1997] and to the south by the Jinshajiang-Ailaoshan-Song Ma (Song Chay) Orogen [e.g., *Faure et al*., 2014] (Figure 1). The eastern margin of the craton extends to the continent-ocean boundary with the South China Sea. The craton consists of the Yangtze Block to the northwest and Cathaysia Block to the southeast, which were assembled in the early Neoproterozoic along the Jiangnan Orogen [*Cawood et al*., 2013; *Li et al*., 2002b, 2007; *Wang and Mo*, 1995; *Wang et al*., 2013b; *Zhao and Cawood*, 2012] (Figure 1). The Yangtze and Cathaysia blocks include Archean and Paleoproterozoic metamorphic basement assemblages and the intervening Jiangnan/Sibao Orogen, which consists of a metaigneous and metasedimentary Neoproterozoic assemblage [*Gao et al*., 1999; *Qiu et al*., 2000; *Zhao and Cawood*, 1999, 2012].

Mid-Neoproterozoic to Paleozoic successions overlie the assembled South China Craton [*Li et al*., 2010; *Yu et al*., 2009, 2010; *Zhao and Cawood*, 2012].

In the Late Carboniferous to the Early Permian, the South China Craton was covered by widespread carbonate deposits including the areas of the Yong'an and Yongjiang basins. Carbonate sedimentation was continuous into the Early Triassic in the Youjiang Basin [*Bureau of Geology and Mineral Resources of Guangxi Zhuang Autonomous Region*, 1985; *Bureau of Geology and Mineral Resources of Fujian Province (BGMRFP)*, 1985; *Bureau of Geology and Mineral Resources of Guangdong Province*, 1988; *Bureau of Geology and Mineral Resources of Hunan Province (BGMRHN)*, 1988] (Figures 2a–2d). In the Middle Permian, the Yong'an Basin was filled with continental shelf-delta front siltstone and sandstone deposits through sediment progradation to the southeast (Figure 2b). In the Late Permian the basin was the site for accumulation of near-shore tidal flat siltstone, mudstone, and carbonate (Figure 2c) whereas along the southern margin of the craton the Qinfang Trough was closed and transformed into a foreland basin (Shiwandashan Basin) (Figure 2c). In the Early Triassic, the Yong'an Basin deepened with detritus sourced from the Wuyi Mountain region and accumulating in a succession of turbidite deposits (Figure 2d). Time equivalent strata in the Shiwandashan Basin received detritus from the Yunkai Massif and material from the southern collision zone of the craton [*Hu et al*., 2015]. In the Middle Triassic most of the southern and eastern regions of the South China Craton underwent uplift and erosion. The Youjiang Basin was transformed into a foreland basin [*Yang et al*., 2012a] (Figure 2e). Sedimentation in the Yong'an Basin was limited to lacustrine deposits in the central and northeast parts of the basin [*BGMRFP*, 1985] (Figure 2e). In Late Triassic to Early Jurassic, the South China Craton was the site of limited molasse deposits, which in the Yong'an Basin accumulated in alluvial fan and fluvial environments [*BGMRFP*, 1985] (Figure 2f).

2.2. Southwest Japan

Proto-Japan originally formed the continental margin of the South China Craton during the separation from Rodinia by rifting at 750–700 Ma [*Isozaki*, 1996; *Isozaki et al*., 2010]. In the Cambrian, Japan was converted from a passive margin to a convergent plate margin and throughout the Paleozoic and Mesozoic constituted an accretionary orogen [*Cawood et al*., 2009; *Isozaki et al*., 2010; *Wakita*, 2013] related to subduction of the Paleo-Pacific beneath the continental margin of the South China Craton (~500 Ma) [*Isozaki and Maruyama*, 1991; *Isozaki et al*., 2010; *Cocks and Torsvik*, 2013]. Pulses of orogenic activity affected the region throughout the Paleozoic and Mesozoic [*Isozaki et al*., 2010]. Precambrian detrital zircons occur in some units implying input from continental sources [e.g., *Fujisaki et al*., 2014; *Sano et al*., 2000; *Wakita*, 2013].

2.3. Yong'an Basin

The Yong'an Basin lies close to the Pacific margin of the South China Craton (Figure 1) and consists of Middle Paleozoic to Cenozoic strata unconformably overlying Precambrian to Early Paleozoic units. Within the basin succession, Upper Triassic-Jurassic strata are unconformable on pre-Middle Triassic strata. Rock units in the basin strike northeast-southwest and the basin is separated from the basement exposed in Wuyi Mountain region to the northwest by the Shaowu-Heyuan fault and from Mesozoic to Cenozoic volcanic rocks to the southeast by the Zhenghe-Dapu fault [*BGMRFP*, 1985; *Zu et al*., 2012] (Figure 3).

The Late Paleozoic to Mesozoic succession in the Yong'an Basin consists of deep marine carbonates of the Lower Permian Qixia Formation passing up into shallow water siliciclastic units of the Wenbishan Formation, which in turn pass into grey bedded mudstones and siltstone of the Middle Permian Tongziyan Formation. This latter unit is disconformably overlain by shallow marine to continental sandstone and siltstone of the Upper Permian Cuipingshan Formation [*BGMRFP*, 1985] (Figures 3–5). The Lower Triassic strata consist of grey calc-siltstones, mudstones, and quartz, mica sandstone with interbedded limestone of the Xikou Formation, which in turn pass up into sandstones of the Xiwei Formation [*BGMRFP*, 1985; *Li et al*., 1997]. The Middle Triassic An'ren Formation, which is mainly restricted to the area around An'ren (Figure 3), consists of medium- to thick-bedded quartzo-feldspathic sandstone, purple mudstone, and siltstone (Figure 5). The Upper Triassic succession comprises the Dakeng and Wenbinshan formations, which unconformity overlie older units. The Dakeng Formation, which is mainly exposed in the north of the study area, consists of quartzo-feldspathic sandstone (Figure 4). The Wenbinshan Formation, present in the center and north of the basin, consists of conglomerate at its base passing up into grey quartz sandstone. Clasts within the conglomerate are up to 20 cm in diameter and consist of quartz-sandstone

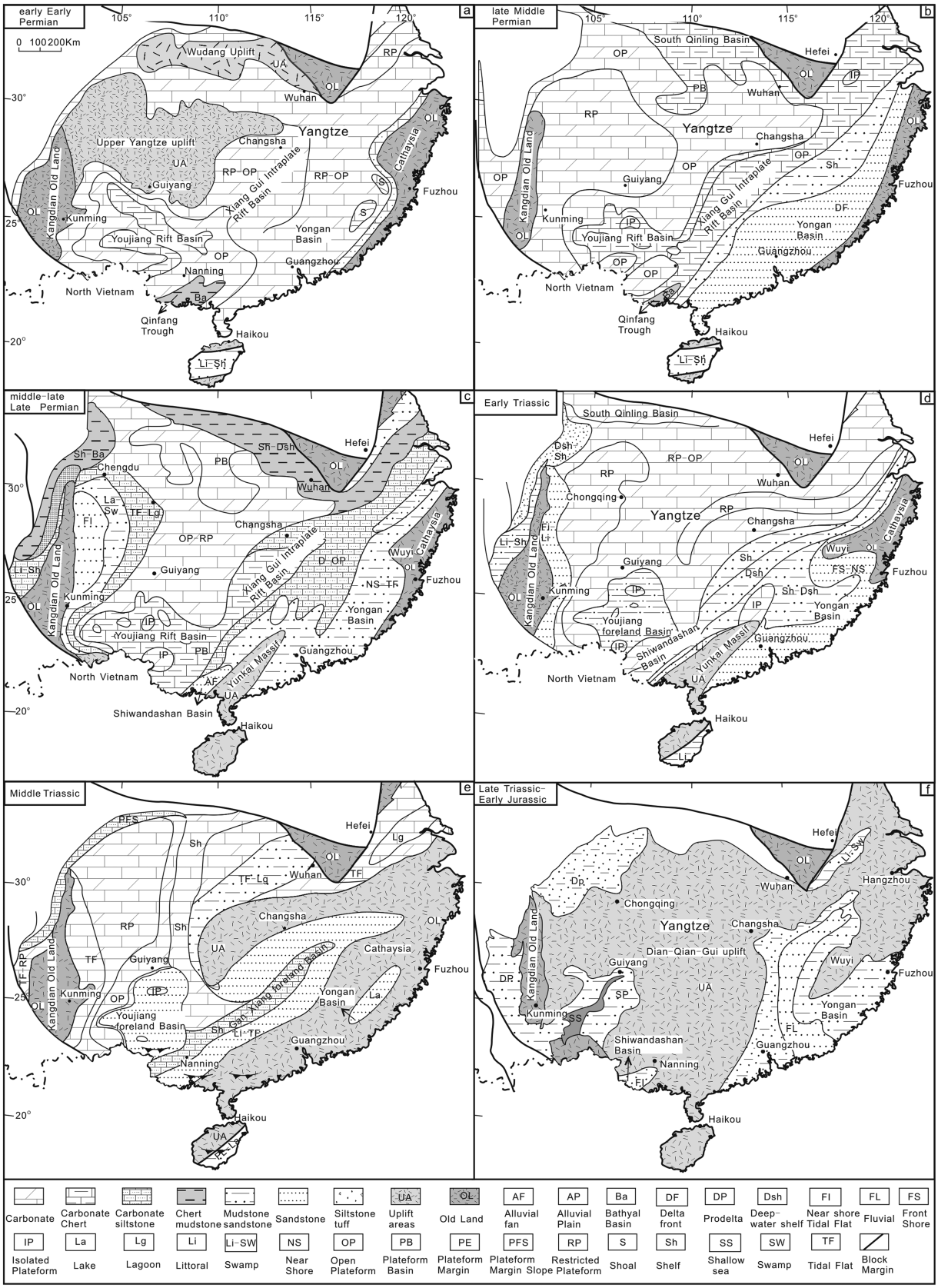

Figure 2. Paleography map of the South China Craton in Permian-Jurassic (modified from *Ma et al.* [2009]).

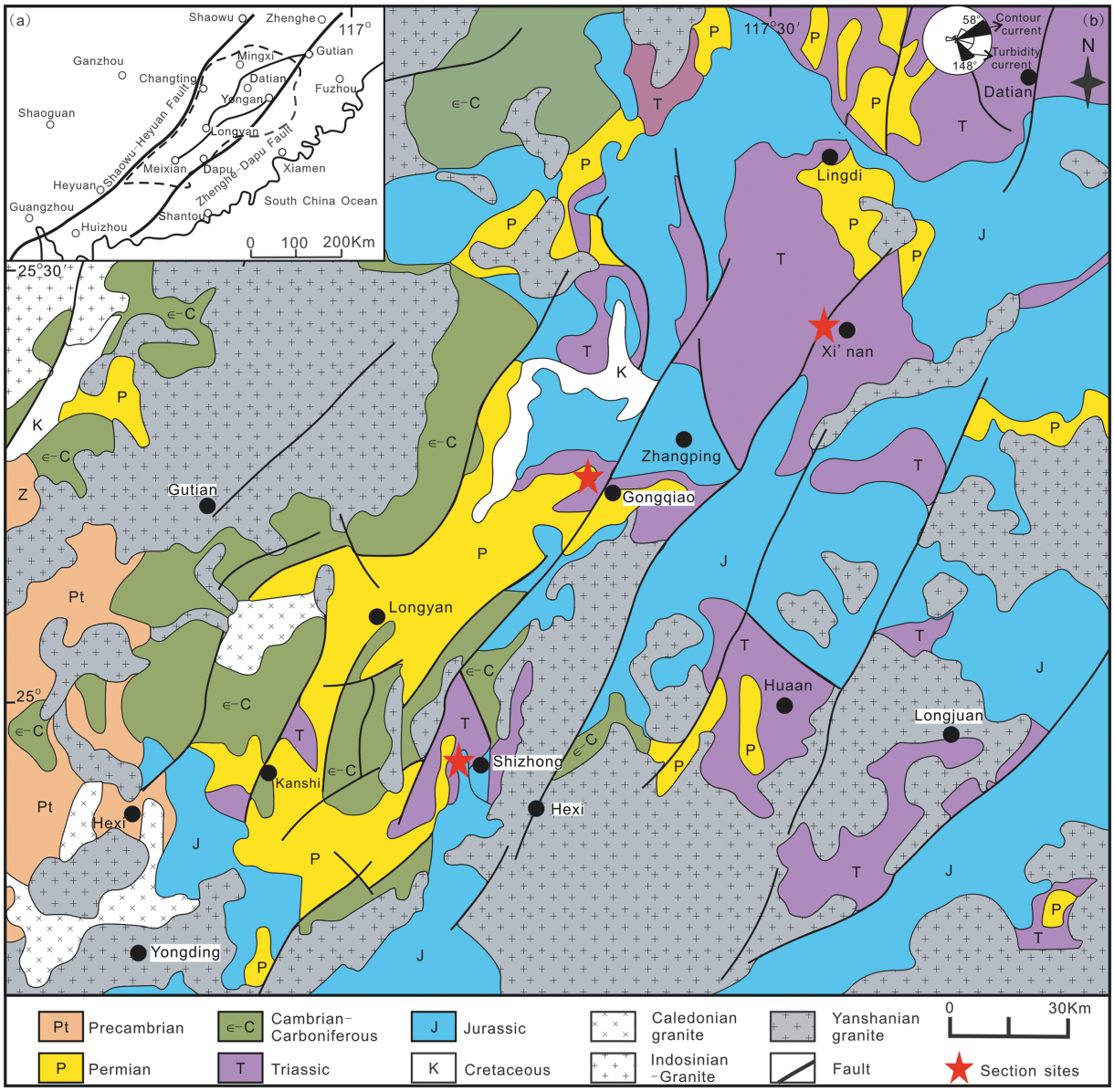

Figure 3. Geological map of the Yong'an Basin (modified from the Fujian geological map) showing the location of sections. Abbreviations: Pt, Precambrian; ∈–C, Cambrian to Carboniferous; P, Permian; T, Triassic; J, Jurassic.

with some limestone, mudstone, and granite (Figures 4 and 5). The conformably overlying Lower Jurassic Lishan Formation consists of conglomerate in the lower part and interstratified sandstone, siltstone, and mudstone in the upper part (Figures 4 and 5). The overlying Middle Jurassic Zhangping Formation comprises purple mudstone and shale within olive green fine sandstones.

3. Sample Setting and Analytical Methods

Samples from the Permian to Jurassic units of the Yong'an Basin were collected from three sections, which from north to south are the Shizhong, Gongqiao, and Xi'nan sections (Figures 3 and 4). The Shizhong and Gongqiao sections comprise Early Jurassic to Late Triassic strata unconformable on Permian to Early Triassic strata whereas the Xi'nan section consists of a continuous Triassic succession (Figure 4). Limited paleocurrent data for the Lower Triassic strata indicate flow from the northwest [*Li et al.*, 1997]. However, sedimentary facies in the Yong'an Basin suggest that areas to the southwest and southeast of the basin could also have acted as potential sources areas in Permian-Jurassic (Figure 2).

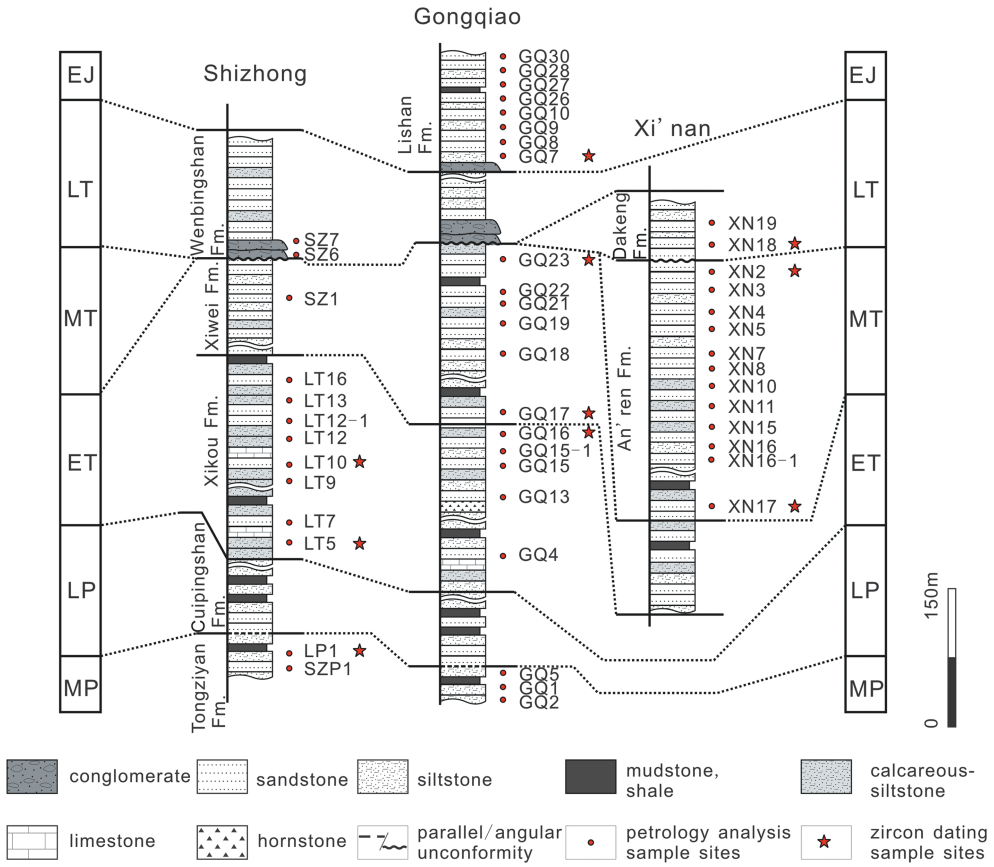

Figure 4. Measured sections through the Permian to Jurassic succession in the Yong'an Basin at Shizhong, Gongqiao, and Xi'nan, showing stratigraphic position of analyzed samples. Abbreviations: MP, Middle Permian; LP, Late Permian; ET, Early Triassic; MT; Middle Triassic; LT, Late Triassic; EJ, Early Jurassic.

Forty-four samples were selected for modal analysis of which 10 were also selected for detrital zircon analysis (Figure 4). Modal analysis is based on the point counting of some 300 points, on grains larger than 60 μm, following the Gazzi-Dickinson method [*Dickinson*, 1985; *Dickinson and Valloni*, 1980; *Dickinson et al*., 1983]. Detail modal results are listed in Data Set S1 in the supporting information. Zircons were separated from sandstone samples using conventional density and magnetic separation techniques, prior to handpicking under a binocular microscope and mounting in epoxy and polishing for backscattered electron (BSE) and cathodoluminescence (CL) imaging. U-Pb ages and trace element analyses on the zircons were determined on an Agilent 7700a at the State Key Laboratory of Geological Processes and Mineral Resources. Analytical procedure follows *Yuan et al*. [2004] and *Liu et al*. [2010]. Zircon standards National Institute of Standards and Technology 610 (NIST610), 91500 and GJ-1, were used to calibrate the U-Th-Pb ratios and absolute U abundances. Off-line selection, integration of background, analytic signals, time-drift correction, and quantitative calibration for U-Pb dating were performed with ICPMSDataCal [*Liu et al*., 2010]. Spot diameter was 32 μm. Error on individual analyses is given at 1 sigma. Common Pb correction was not performed as U-Pb ages are concordant or nearly concordant. For rare earth element (REE) analyses the average analytical error ranges from approximately ± 10% for light rare earth elements (LREE) to approximately ± 5% for the other REE. Zircon U-Pb age concordance is defined as 100 × (1-abs ($^{206}Pb/^{238}U$ Age-$^{207}Pb/^{235}U$ Age)/$^{206}Pb/^{238}U$). The Laser Ablation Inductively Coupled Plasma Mass Spectrometry (LA-ICP-MS) U-Pb isotopic age and trace element analyzes results are listed in Data Sets S2 and S3. All analyses are plotted on concordia diagrams (Figure S1), but only analyses with concordance ≧90 are incorporated in the combined probability density and histogram plots and discussed in the text. Age and probability density plots are calculated using the Isoplot program 3.0 [*Ludwig*, 2003]. In order to reduce the effect of Pb loss, ages older than 1000 Ma are based on $^{207}Pb/^{206}Pb$ ages whereas for younger analyses they are based on $^{206}Pb/^{238}U$ ages [*Compston et al*., 1992].

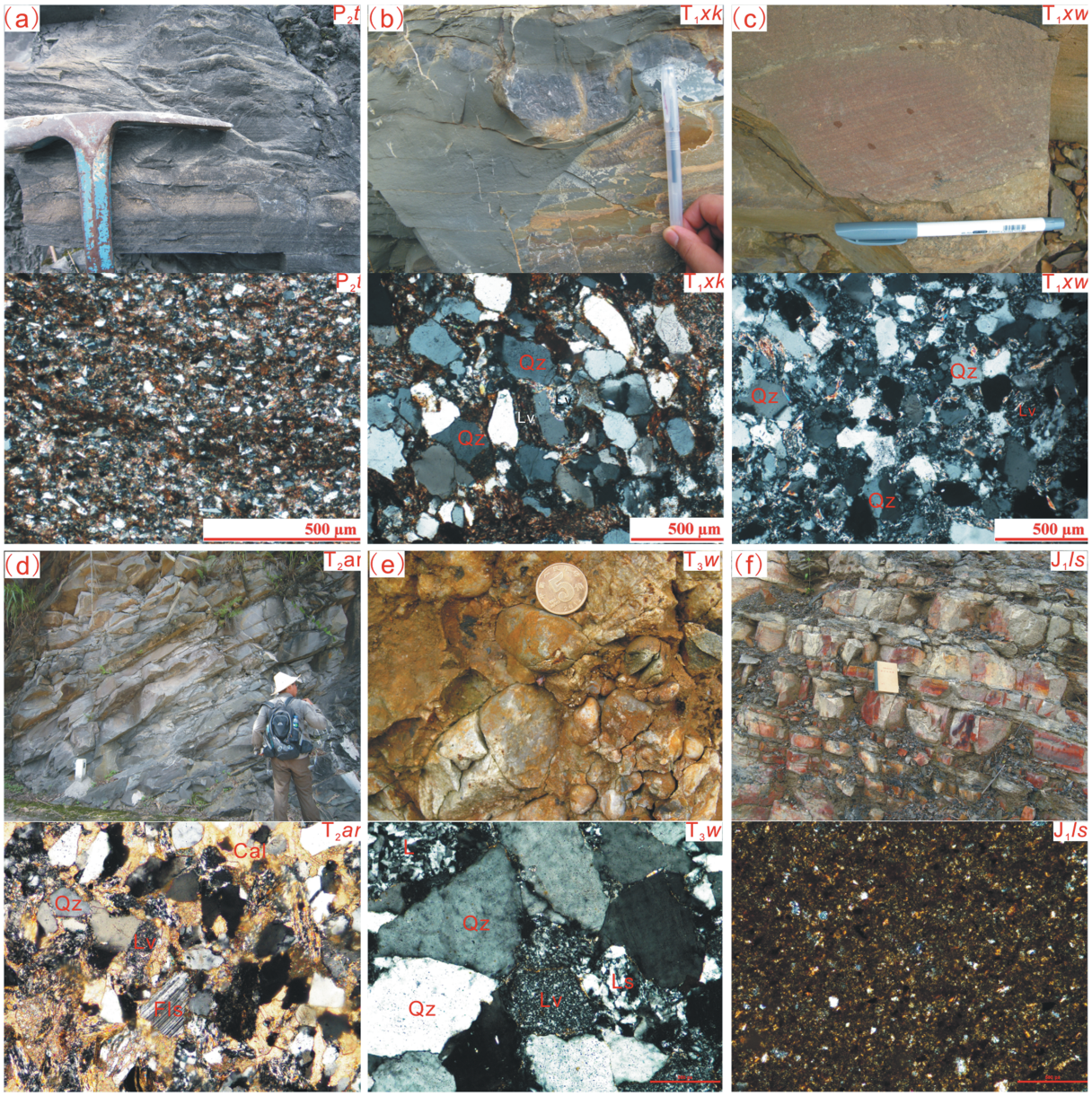

Figure 5. Field photographs and photomicrographs of the Permian-Jurassic succession in the Yong'an Basin, (a) siltstone of Middle Permian Tongziyan Formation, Shizhong section; (b) grey siltstone of Lower Triassic Xikou Formation, Shizhong section; (c) brown sandstone of Lower Triassic Xiwei Formation, Gongqiao section; (d) conglomerate of Upper Triassic Wenbinshan Formation, Gongqiao section; (e) siltstone of Middle Permian Tongziyan Formation, Gongqiao section; (f) sandstone of Lower Triassic Xikou Formation, Gongqiao section; (d) sandstone of Middle Triassic An'ren Formation, Xi'nan section; (e) conglomerate of Upper Triassic Wenbinshan Formation, Gongqiao section; and (f) grey sandstone within siltstone of Lower Jurassic Lishan Formation, Gongqiao section. Abbreviations: Cal, calcite; Ls, sedimentary lithic fragment; Lv, volcanic lithic fragment; Qz, quartz grain; Fs, feldspar.

4. Results

4.1. Petrography and Modal Analysis

The major detrital component is monocrystalline quartz along with variable but minor amounts of polycrystalline quartz, plagioclase feldspar, lithic fragments (generally sedimentary or volcanic), and mica with limited accessory grains (zircon and apatite). Chlorite resulting from low-grade alteration of matrix is present in minor amounts in most samples, and secondary calcite cement was noted in some samples (Figure 5).

Siltstone samples from the Upper Permian Tongziyan Formation contain angular-subangular detritus around 0.1 mm in diameter. The major components are monocrystalline quartz (80.9%–89.0%) and lithic fragments

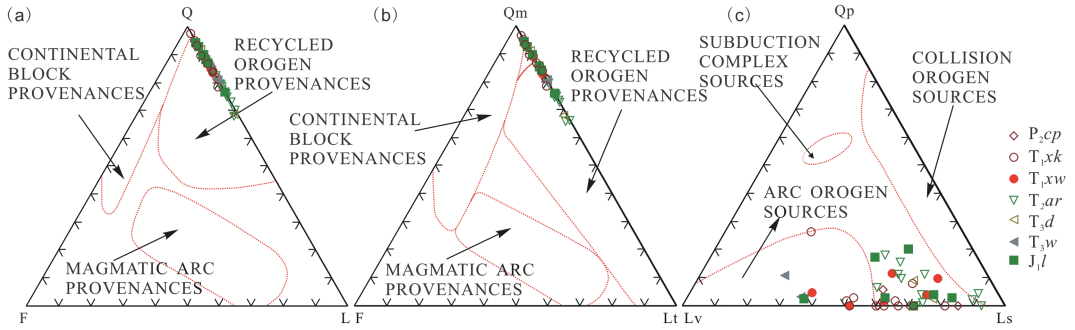

Figure 6. (a) QFL, (b) QmFLt, and (c) QpLvLs diagrams for Permian-Jurassic samples in the Yong'an Basin [after *Dickinson and Suczek*, 1979; *Dickinson et al.*, 1983]. Abbreviations: Q, total quartz; F, total feldspar; L, lithic fragment; Qm, monocrystalline quartz; Qp, polycrystalline quartz; Lv, volcanic lithic fragment; Ls, sedimentary lithic fragment; Lt = L + Qp.

including sedimentary and volcanic grains (6.4%–16.3% and 2.8%–6.3%, respectively). Polycrystalline quartz (0–0.6%) and feldspar (0–0.3%) are minor components in the samples. Samples from the Lower Triassic Xikou Formation are similar to Upper Permian samples and dominated by monocrystalline quartz (78.5%–96.6%) with minor lithic fragments (2.5%–20.3%; average 11.6%) and trace amounts of polycrystalline quartz and feldspar. In places the matrix is replaced by calcite cement. Sandstones from the Lower Triassic Xiwei Formation consist of moderately sorted, subangular to angular, detrital grains. Monocrystalline quartz ranges from 82.8% to 88.8% (average 85.0%), polycrystalline quartz from 0 to 1.2%, and lithic fragments from 9.9% to 16.2%. One sample contains minor feldspar grains (0.3%). Mica occurs in accessory amounts in the Lower Triassic samples. Middle Triassic An'ren Formation sandstones are well sorted with subangular detrital grains, and the major framework components are monocrystalline quartz (65.7%–85.7%; average 75.6%), polycrystalline quartz (0–4.8%; average 1.8%), feldspar (0–1.5%; average 0.2%), and lithic fragments (13.7%–30.7%; average 22.4%). The lithic grains are dominated by sedimentary fragments (12.8%–23.1%; average 16.8%) and volcanic fragments (0.9%–12%; average of 5.6%) and have a diameter of around 0.5 mm. Most of the An'ren Formation samples contain calcite cement as well as minor detrital carbonate grains. The Upper Triassic Dakeng Formation sandstones are similar to the An'ren Formation samples and consist of monocrystalline quartz (67.6%–90.9%; average 79.3%), polycrystalline quartz (0.8%), feldspar (0.0%–1.1%; average 0.5%), and lithic fragments (8.3%–30.2%; average 19.3%). Conglomerate clasts from the Upper Triassic Wenbinshan Formation range from 2 to 30 cm and include sandstone, quartzite, limestone, and granite. The sandstones of the Wenbinshan Formation are composed almost entirely of monocrystalline quartz with little other framework grains. Siltstone samples from Lower Jurassic Lishan Formation contain angular to subangular grains ranging from 0.1 to 0.2 mm and mainly consist of monocrystalline quartz and lithic fragments. A summary of modal results is listed in Data Set S1 and plotted on Q-F-L and Qm-F-Lt diagrams [*Dickinson and Suczek*, 1979; *Dickinson et al.*, 1983]. The analyzed samples fall within or close to the recycled-orogen field on the Q-F-L diagram (Figures 6a and 6b), whereas on the Qp-Lv-Ls diagram they lie along or close to the Lv-Ls tie and largely between the collisional orogen and arc orogen sources (Figure 6c).

4.2. Detrital Zircon Analysis

Zircons from analyzed samples in the Yong'an Basin are transparent to semitransparent, subhedral to occasionally rounded. Zircons from LP1, LT5, and LT10 are 30–50 μm in length whereas in the other samples they range from 50 to 150 μm (Figure S2). Most grains show oscillatory zoning and sector structure in cathodoluminescence (CL) images and a few display core-rim and homogeneous structures (Figure S2).

4.2.1. Middle Permian Sample

Fifty-four analyzes on 54 detrital zircon grains were undertaken on sample LP1 from the Middle Permian Tongziyan Formation, Shizhong section. Forty analyses ages displayed concordance greater than 90% and are dominated by age groups at 2000–1700 Ma, 900–700 Ma, and 300–250 Ma and minor groups at 1200–900 Ma, 650–480 Ma, 460–420 Ma, and 400–340 Ma (Table S1 and Figure 7).

4.2.2. Lower Triassic Samples

Two hundred and twenty-five spots were analyzed from three samples (LT5, LT10, and GQ16) of the Xikou Formation, 206 yield concordant ages that range from 3500 to 280 Ma. Major age groups occur at 2000–1700 Ma, 1200–900 Ma, and 460–420 Ma. Sample GQ16 also displays a major age group at 400–340 Ma (Table S1 and Figure 7).

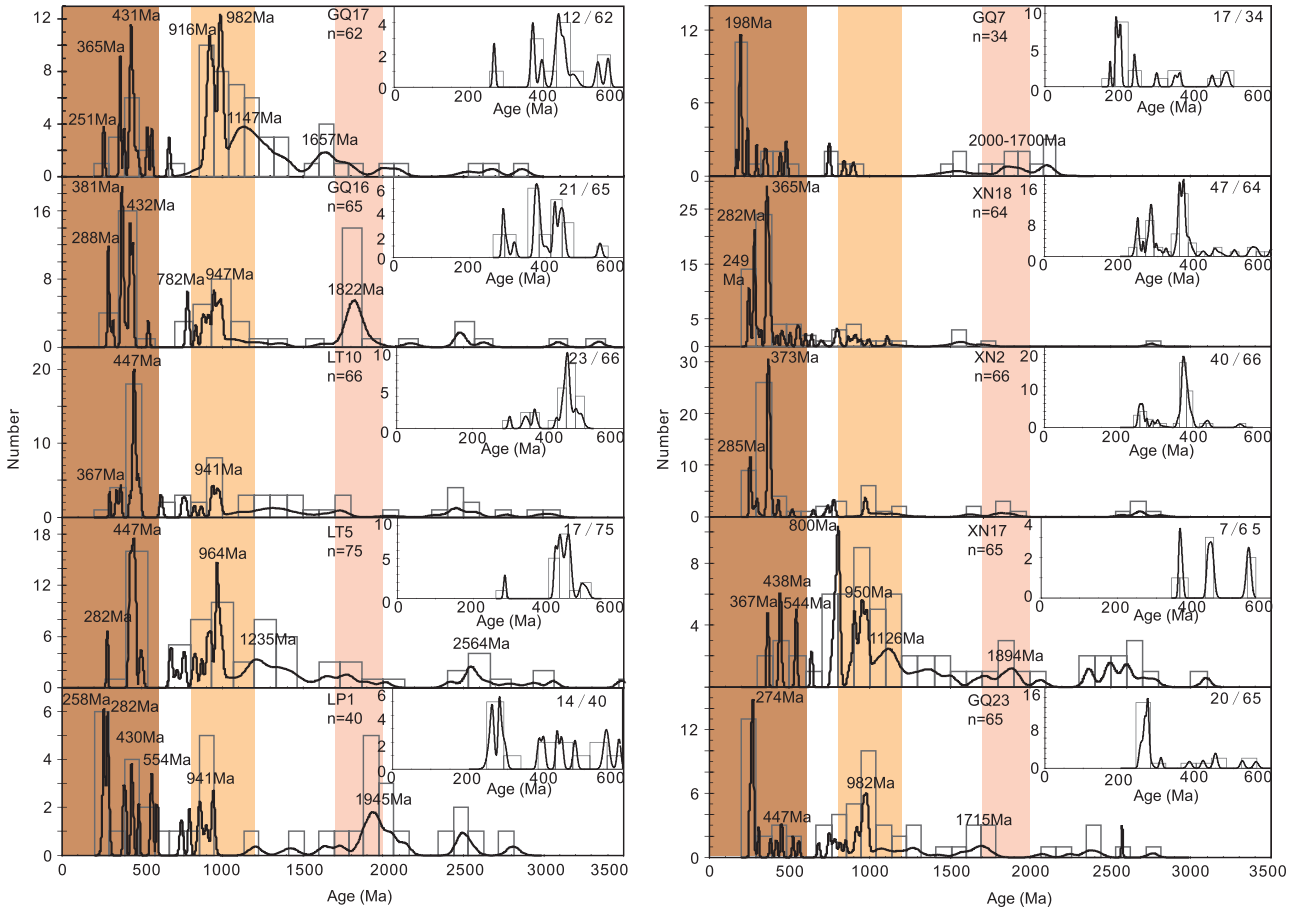

Figure 7. LA-ICP-MS zircon U-Pb age histograms of detrital zircons from Permian-Jurassic samples in the Yong'an Basin.

Two samples, GQ17 and GQ23, from the Xiwei Formation, Gongqiao section, yielded 127 out of a total of 132 analyses that display concordance greater than 90% and range in age from 2900 Ma to 240 Ma. Major age groups are 2000–1700 Ma, 1200–900 Ma, and 280–240 Ma with subordinate groups at 900–700 Ma, 460–420 Ma, and 400–340 Ma (Table S1 and Figure 7).

4.2.3. Middle Triassic Samples

Two samples (XN2 and XN17) from the An'ren Formation in the Xi'nan section were analyzed. All 131 analyses yielded concordance greater than 90% and range in age from 3100 to 240 Ma. Major age groups occur at 1200–900 Ma and 900–700 Ma in sample XN17 and 1200–900 Ma, 400–350 Ma, and 300–240 Ma in sample XN2, respectively (Table S1 and Figure 7).

4.2.4. Upper Triassic Samples

Sixty-six U-Pb detrital zircon analyses for sample XN18 from the Dakeng Formation and 64 analyses yielded concordance greater than 90% and range in age from 2800 Ma to 240 Ma. The major age groups are 400–340 Ma and 300–250 Ma with minor age groups at 2000–1700 Ma, 1200–900 Ma, 900–700 Ma, 650–480 Ma, 460–420 Ma, 350–300 Ma, and 250–210 Ma (Table S1 and Figure 7).

4.2.5. Lower Jurassic Samples

Sixty analyses on 58 zircon grains were analyzed from Lower Jurassic sample GQ7. Only 34 yielded concordant ages, which fall in the range of 2128 Ma to 172 Ma. The sample is characterized by two major groups at 2000–1700 Ma and 200–180 Ma with a scattering of points at 1700–1400 Ma, 900–700 Ma, and 500–200 Ma (Table S1 and Figure 7).

4.3. The Zircon Trace Elements

LA-ICP-MS trace element data for the analyzed detrital zircons are listed in Data Set S3. Most grains display well-developed prismatic crystal morphology and oscillatory zoned CL images, with high Th/U ratios

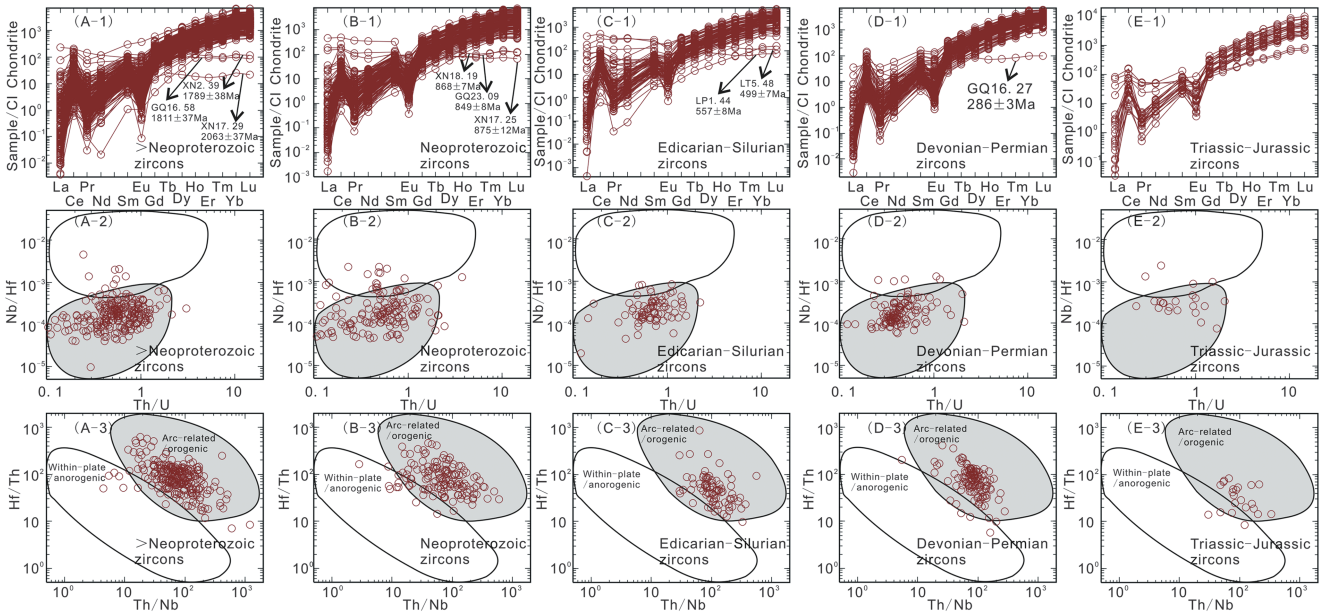

Figure 8. (A-1, B-1, C-1, D-1, and E-1) CI Chondrite-normalized REE patterns, spider diagrams for the detrital zircons of the Permian-Jurassic samples in the Yong'an Basin (CI Chondrite data are from *Sun and McDonough* [1989]); (A-2, B-2, C-2, D-2, E-2; A-3, B-3, C-3, D-3, and E-3) Zircon trace element Th/U versus Nb/Hf and Th/Nb versus Hf/Th, diagram of the Permian-Jurassic samples in the Yong'an Basin, respectively (according to *Yang et al.* [2012b]).

(most > 0.1) and characterized by typically steep chondrite normalized REE pattern (Gd_N/Yb_N = 0.01–0.21) with positive Ce (>2) and negative Eu (<0.2) anomalies (Figure 8). These characteristics are consistent with a magmatic origin [*Hoskin and Ireland*, 2000; *Hoskin and Schaltegger*, 2003]. CL images of some older grains (>500 Ma) display homogeneous dark grains or planar oscillatory zoned grains overgrown by a discontinuous light and bright rim. These characteristics combined with their low Th/U ratio (0.02–0.27) and flat heavy rare earth element (HREE) pattern, suggests a metamorphic origin [*Hoskin and Ireland*, 2000; *Hoskin and Schaltegger*, 2003] (Figures S2 and 8). One of these grains dated at 557 ± 8 Ma (LP1.44) is characterized by a low Th/U (0.09), very high U/Nb (713), a chondrite normalized flat HREE pattern (Gd_N/Yb_N = 0.58), a very small Eu anomaly (Eu/Eu* = 0.78), and a positive Ce anomaly (Figure 8; Ce/Ce* = 8.86). Combined with the homogeneous dark CL image (Figure S2), this grain (LP1.44) is interpreted to have formed under eclogite-facies metamorphic conditions [*Wu et al.*, 2009, and references therein]. Other probable metamorphic zircon grains have flat chondrite normalized HREE pattern (Gd_N/Yb_N = 0.33–1.99), high U/Nb (53–1349), and a positive Ce anomaly (Ce/Ce* = 3.71–75.3), but with a strong Eu anomaly (Eu/Eu* = 0.01–0.35), consistent with a granulite-facies metamorphic source [*Wu et al.*, 2008] (Figure 8).

All analyzed igneous detrital zircon grains from the Yong'an Basin were plotted on Th/U versus Nb/Hf and Th/Nb versus Hf/Th diagrams which differentiate an extensional within-plate (anorogenic environment) from a compressional magmatic arc (orogenic) setting [*Yang et al.*, 2012b] (Figure 8). The majority of analyses lie in the arc-related/orogenic field with a few grains falling into the within-plate/anorogenic field, suggesting that potential sources are dominated by magmatic rocks formed in a convergent environment (Figure 8).

5. Discussion

5.1. Provenance of Pre-Middle Paleozoic Detrital Zircons

Potential source regions for detrital zircons with ages greater than 400 Ma from the Permian to Jurassic samples of the Yong'an Basin likely occur within the South China Craton. Archean and Paleoproterozoic detrital zircon grains (circa >2.0 Ga), which are mainly present in the Permian to Early Triassic samples, are generally oval in shape with pitted, abraded surfaces (Figure S2), indicating long-distance transport from their source and/or multicycled sedimentary processing. Archean rocks are present within the Yangtze Block [*Gao et al.*, 1999; *Qiu et al.*, 2000; *Zhao and Cawood*, 2012]; however, during Permian to Early Triassic,

the Yangtze Block was covered by carbonate deposits and could not have been a potential source for this detritus. Thus, Archean grains in the samples are inferred to have been reworked material of this age that occurs in Neoproterozoic to Early Paleozoic sedimentary successions on the South China Craton.

Late Paleoproterozoic (circa 2.0–1.7 Ga) zircons are present in all samples and constitute major age groups in samples LP1, GQ7, GQ16, and XN17 (Table S1 and Figure 7). Most of these zircons are subhedral to euhedral crystals suggesting minimal transport from source. They show oscillatory zoning under CL, and their Th/U ratios are indicative of a magmatic origin, except grains XN2.39 (1789 ± 38 Ma) and GQ16.58 (1811 ± 27 Ma), which display features indicative of a metamorphic origin (Figure 8). Late Paleoproterozoic magmatic rocks (circa 2.0–1.7 Ga) are widespread in the Wuyi Mountain region, immediately northwest-north of the Yong'an Basin [*Li*, 1997; *Liu et al*., 2009; *Xia et al*., 2012; *Xiang et al*., 2008; *Yu et al*., 2012, 2009] and metamorphic rocks of this age are also reported from this region [*Yu et al*., 2012, 2009], consistent with the paleocurrent and sedimentary facies data from the Yong'an Basin (Figure 2).

Late Mesoproterozoic to early Neoproterozoic (circa 1.2–0.9 Ma) zircon grains constitute a major age group in Lower to early Middle Triassic samples and a component in late Middle to Upper Triassic samples (Table S1 and Figure 7). Crystal shapes range from rounded to euhedral crystals. Early Neoproterozoic magmatic rocks are exposed in the Wuyi Mountain region, Yunkai Massif, and along the Jiangnan orogen, and grains of this age, along with late Mesoproterozoic aged grains, also occur in the Early Paleozoic sedimentary rocks [*Wang et al*., 2010, 2013b; *Zhang et al*., 2012; *Zhao and Cawood*, 2012; *Yao et al*., 2014, 2015a, 2015b]. Early Neoproterozoic aged rocks in the Jiangnan Orogen are unlikely to have acted as a source as this region was covered by the Late Paleozoic carbonate succession (Figure 2). Thus, we inferred that the euhedral grains were derived from primary magmatic rocks in the Wuyi Mountain and Yunkai Massif whereas the subhedral to rounded grains could have been recycled from adjoining sedimentary units.

Detrital zircon grains with ages 900–700 Ma and 650–500 Ma occur as a minor component of all samples and ages 900–700 Ma also occur as a major component of sample XN17 (Table S1 and Figure 7). Apart from grains XN17.23 (875 ± 12 Ma), XN18.19 (868 ± 7 Ma), GQ23.09 (849 ± 8 Ma), and GQ16.27 (834 ± 8 Ma), which show features indicative of a metamorphic origin (probably from a high-grade granulite facies source), the remaining grains with these ages display magmatic zircon patterns (section 4.3 and Figure 8). Magmatic and metamorphic rocks in the range 900–700 Ma occur on the southeastern and western margin of the Yangtze Block (Jiangnan and Panxi-Hanan orogenic belts) and sporadically in the Wuyi Mountain region [*Cawood et al*., 2013; *Li et al*., 2008a, 2008b, 2008c; *Ling et al*., 2003; *Wan et al*., 2007; *Zhao and Cawood*, 2012; *Zhou et al*., 2007]. Combined with the paleogeographic and sedimentary facies data for the South China Craton, the Jiangnan and Panxi-Hannan orogenic belts were likely covered by Permo-Triassic carbonate deposits in the central Yangtze Block [*Bureau of Geology and Mineral Resources of Guizhou Province*, 1987; *BGMRHN*, 1988; *Bureau of Geology and Mineral Resources of Sichuan Province*, 1991] and could not supply detritus for the Yong'an Basin in Permo-Triassic. The Wuyi Mountain region was the potential source area as the paleocurrents flow from northwest, and the paleogeographic reconstruction is also consistent with derivation from such a source (Figure 2). Detrital zircons in the range 650–500 Ma have no known igneous or metamorphic source rocks in the South China Craton. The majority of these detrital grains are from original igneous sources but at least two are from high-grade metamorphic sources; grain LP1.44 (557 ± 8 Ma) has features suggesting derivation from an eclogite-facies source and LT5.48 (499 ± 7 Ma) from a granulite source (Figure 8). However, detritus with ages in the range 650–500 Ma occur in Early Paleozoic sedimentary strata in the South China Craton and are inferred to have originally been derived from the SE, beyond the limits of the craton, and from sources associated with Gondwana assembly [*Cawood and Nemchin*, 2000; *Cawood et al*., 2013; *Myrow et al*., 2010; *Wang et al*., 2010; *Xu et al*., 2014, 2013; *Yao et al*., 2014, 2015a, 2015b]. Erosion of this Early Paleozoic succession has been invoked as source in other Late Paleozoic to Early Mesozoic basins in South China [e.g., *Hu et al*., 2014, 2015] and thus could have also supplied detritus to the Yong'an Basin.

Early Paleozoic (460–420 Ma) detrital zircon grains are mainly preserved in the Lower Triassic samples and display subhedral to euhedral crystal form, indicating short transport from their source area(s). These detrital zircons show CL image and REE patterns indicating a magmatic origin, consistent with the widespread Early Paleozoic granitic rocks in the nearby Wuyi Mountain region [*Li et al*., 2010; *Wang et al*., 2013a] (Figure 9). In summary, magmatic and metamorphic rocks in the Wuyi Mountain region, and Yunkai Massif, together with recycled detritus in Early Paleozoic strata around the basin are likely the main sources for Precambrian to Early Paleozoic detritus in the Permian-Jurassic successions of the Yong'an Basin.

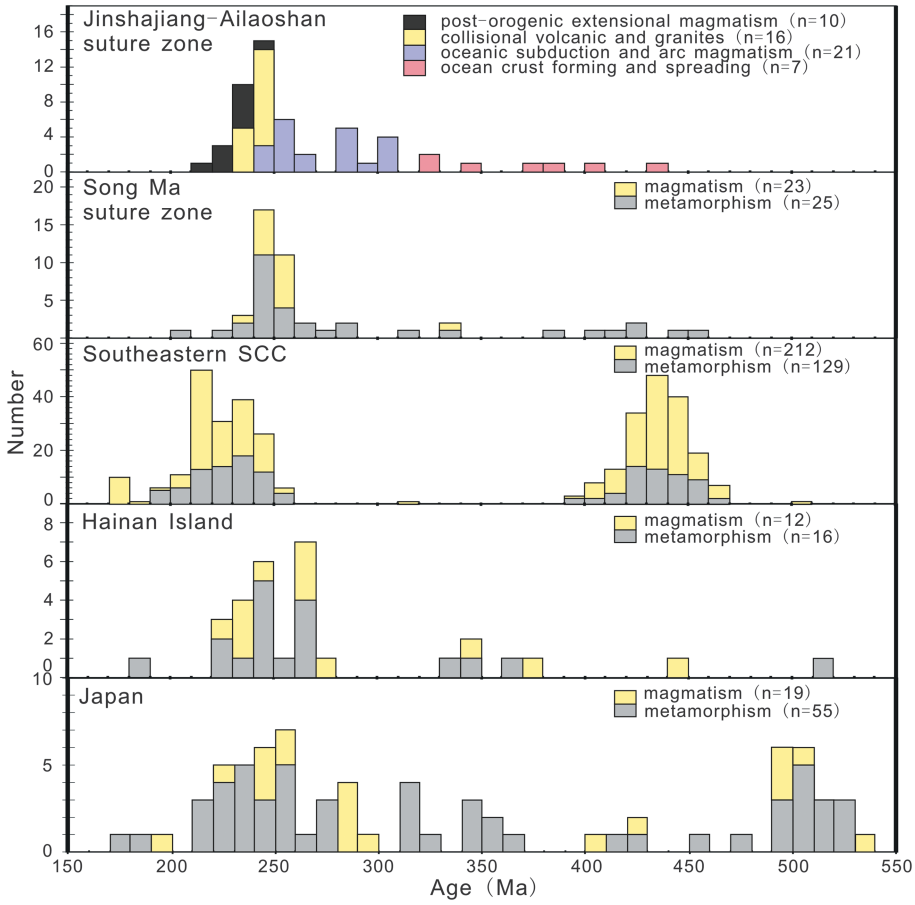

Figure 9. Histograms summarizing published zircon U-Pb ages of major magmatic and tectonothermal events in the Jinshajiang-Ailaoshan suture zone, Song Ma suture zone, southeast South China Craton (Cathaysia Block), Hainan Island, and southwest Japan magmatic zircon age were largely obtained by sensitive high-resolution ion microprobe (SHRIMP) and LA-ICP-MS analysis, with minor data from whole rock Sm-Nd analysis; metamorphic events are obtained by SHRIMP, LA-ICP-MS, mica Ar-Ar analysis, and whole rock Sm-Nd analysis. Data sources: Jinshajiang-Ailshan zone = *Zi et al*. [2013, and references therein] and *Jian et al*. [2009a, and references therein; 2009b]; Song Ma zone = *Faure et al*. [2014], *Carter et al*. [2001], *Nagy et al*. [2001], *Osanai et al*. [2004], *Nam et al*. [2001], and *Tran et al*. [2008]; Southeast SCC = *Meng et al*. [2012], *Wang et al*. [2013a, and references therein], and *Yu et al*. [2013]; Hainan Island = *Chen et al*. [2006, 2013, 2011], *Ding et al*. [2005], *Li et al*. [2002a, 2002b, 2006, 2005], *Xie et al*. [2006, 2005], *Tang et al*. [2013], *Zhang et al*. [2011], and *Xu et al*. [2007, 2006]; southwest Japan = *Horie et al*. [2010], *Takahashi et al*. [2010], *Sakashima et al*. [2003, and references therein], *Herzig et al*. [1997], *Fujii et al*. [2008], *Tagiri et al*. [2011, and references therein], *Takayuki et al*. [2008], *Sano* [1992], *Igi et al*. [1979], *Ishiwatari and Tsujimori* [2003, and references therein], *Tsujimori and Itaya* [1999], *Tsujimori et al.* [2006, and references therein], *Tsutsumi et al*. [2010], and *Osanai et al*. [2006, and references therein].

5.2. Provenance of Middle Paleozoic to Early Mesozoic (400–170 Ma) Detrital Zircons

Paleozoic (400–250 Ma) zircon grains occur in all samples (Table S1 and Figure 7). Most are euhedral (Figure S2), suggesting short distance transport from source (Figure 5). There are practically no magmatic and metamorphic rocks with these ages exposed in the mainland portion of the South China Craton. Granite with an age of circa 380 Ma occurs in NW Hunan in the Yangtze Block, west of the Jiangnan orogen [*Zhao et al*., 2013], but this region was the site of carbonate accumulation during the Permian to Early Triassic (Figure 2) and thus would not have constituted an exposed source. This information, combined with both southeast and northwest trending paleocurrents preserved in Lower Triassic strata [*Li et al*., 1997], suggest that the Middle Paleozoic to Permian detritus were likely sourced from beyond east-southeast coastal region of the craton. Limited Late Devonian granite (370 Ma), andesite (345 Ma), and Early to middle Permian granite (270–260 Ma) occur on Hainan Island [*Chen et al*., 2013; *Ding et al*., 2005; *Li et al*., 2006, 2002a, 2002b] (Figure 9) and could have acted as a source for detritus. However, the outcrop area of the rocks on Hainan Island is extremely limited and unlikely that they alone could provide the abundant 400–250 Ma detrital zircons in the analyzed samples.

Japan could also have acted as a source for the Paleozoic grains in the Permian-Jurassic succession in the Yong'an Basin. Rocks of appropriate age include circa 380–340 Ma metamorphic rocks in South Kitakami Belt, 340–280 Ma high-P/T (Pressure/temperature) accretionary complex (Renge and Oki belts), 290–210 Ma granite (Hida, Akiyoshi, Maizuru, Ultra-Tamba, and Kurosegawa belts), and 260 Ma accretionary complex (Akiyoshi belt) [*Fujii et al*., 2008; *Herzig et al*., 1997; *Ishiwatari and Tsujimori*, 2003; *Sakashima et al*., 2003; *Tagiri et al*., 2011; *Uchino et al*., 2008; *Wakita*, 2013] (Figure 9). Furthermore, Lower Carboniferous strata in Japan contain extensive detrital zircon grains in the range 400–340 Ma and could also have acted as a source for detritus of this age [*Isozaki et al*., 2014] (Figures 10 and 11). Although Japan currently lies to the north-northeast of South China and no paleocurrents in the Permian-Jurassic strata of the Yong'an Basin indicate a source in this region, recent work suggests Japan was linked to South China in Late Paleozoic to early Mesozoic [*Isozaki et al*., 2010, 2014; *Uno et al*., 2011]. Evidence supporting this link includes the following: (1) Japan and the South China Craton that show faunal similarities, especially with respect to Permian biostratigraphy (Cathaysian province) [*Ishiga*, 1990; *Kuwahara et al*., 1998; *Nakae and Kurihara*, 2011; *Shi*, 2006; *Sugamori*, 2011; *Wang and Yang*, 2011; *Wang et al*., 2006]; (2) Late Triassic and Jurassic conglomerates in the northeast Japan comprise material inferred to be derived from the South China Craton [*Fujisaki et al*., 2014; *Nutman et al*., 2006]. For example, Jurassic strata in the Yong'an Basin and Northeast Japan terrane display similar detrital zircon age patterns suggesting a common source [*Fujisaki et al*., 2014, and this study] (Figures 10 and 11); and (3) new paleomagnetic data for the Kurosegawa terrane in southwest Japan indicates Japan formed the easternmost element of South China and was subsequently translated ~1500 km northward from the continental margin to its present position in middle to Late Cretaceous [*Uno et al*., 2011]. On the basis of seismic reflection profiles, the distribution of high-P/T metamorphic rocks and detrital zircon chronology data in Japan, *Isozaki et al*. [2010, 2014] has proposed that in Paleozoic-Mesozoic the South China Craton extended farther to the east and Japan is one segment of this "extended craton." Also, the Cathaysian Block was likely more widespread at that time but was removed through multiple episodes of subduction erosion during the Late Paleozoic and Early Mesozoic [*Isozaki et al*., 2010, 2014]. An additional, albeit it is limited, piece of data to support a Japan-South China link is provided by one zircon grain in sample XN18, which shows core (XN18.40) and mantle/rim (XN18.39) ages of Ediacaran (563 ± 5 Ma) and Late Carboniferous (322 ± 4 Ma), respectively. Late Carboniferous (circa 313 Ma) granite are recorded in the South China Craton, but no igneous rocks of Ediacaran age are known [*Yu et al*., 2013] (Figure 9). However, rocks that record the combination of these two ages are present in Japan [*Igi et al*., 1979; *Sano*, 1992; *Sano et al*., 2000; *Takayuki et al*., 2008; *Tsujimori and Itaya*, 1999] (Figure 9).

An alternative possible source for zircons with ages in the range 400–250 Ma is the Jinshajiang-Ailaoshan suture zone along the southwestern margin of South China, which formed in response to subduction and closure of the Paleo-Tethys [*Jian et al*., 2009a, 2009b; *Zi et al*., 2013] (Figure 9). However, this region is far removed from Yong'an Basin and hence not easily reconciled with the pronounced euhedral crystals of 400–250 Ma detrital zircons. In addition, intervening basins between the Yong'an and the suture zone contain little detritus of this age. For example, circa 400–340 Ma detrital zircon grains are a minor component in the Middle Triassic samples of the Youjiang Basin and along with Early to Middle Permian zircon grains (300–260 Ma) are rare in the Permo-Triassic succession of the Shiwandashan Basin (Figures 10 and 11). Thus, the Middle to Late Paleozoic (400–250 Ma) detrital zircons in the Middle Permian and Triassic to Early Jurassic samples in the Yong'an Basin are likely derived from a source located southeast of current limits of the craton.

Triassic (circa 250–210 Ma) detrital zircons mainly occur in the Upper Triassic and Jurassic samples, with a major age peak at ~240 Ma. These zircons are euhedral, with oscillatory zoning, high Th/U ratios, and REE patterns indicative of a magmatic source, consistent with derivation from nearby magmatic rocks. Indosinian granites are widespread in the southeast of the South China Craton and also in southwest Japan and are the likely source for this material [*Li and Li*, 2007; *Takahashi et al*., 2010; *Wang et al*., 2005, 2013a] (Figure 9).

Zircons in the range circa 210–170 Ma in the Early Jurassic sample have a euhedral shape, are oscillatory zoned with high Th/U ratios, and display high chondrite normalized REE contents with steep HREE and a large Eu anomaly, indicating a nearby magmatic source. Jurassic intrusive and volcanic rocks are widespread across the southeast coastal parts of the craton [*Li and Li*, 2007; *Meng et al*., 2012; *Wang et al*., 2013a, 2003] (Figure 9) and are the inferred source for these grains in the Early Jurassic sedimentary rocks.

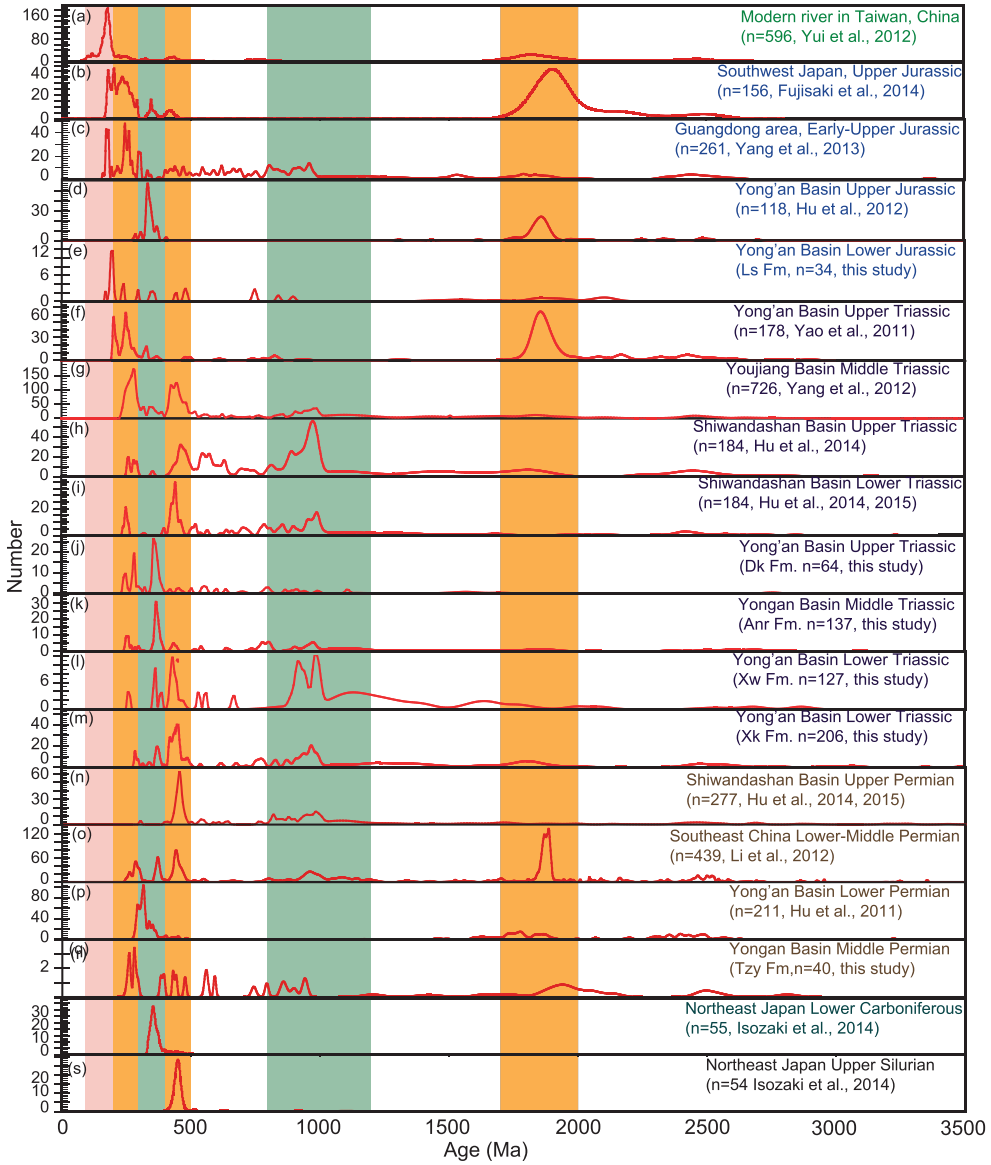

Figure 10. Probability density diagram comparing analyzed detrital zircons in the Yong'an Basin and detrital zircon age of contemporary succession in the SCC [*Hu et al.*, 2014, 2015, 2011; *Li et al.*, 2012; *Yang et al.*, 2012a, 2013; *Yang*, 2013; *Yao et al.*, 2011] and Southwest Japan [*Fujisaki et al.*, 2014; *Isozaki et al.*, 2014]. Abbreviations: Tzy Fm, Tongziyan Formation; Xk Fm, Xikou Formation; Xw Fm, Xiwei Formation; Anr Fm, Anren Formation; Dk Fm, Dakeng Formation; Ls Fm, Lishan Formation.

In summary, an accretionary orogen, which likely incorporated Japan and Hainan Island, was probably situated immediately outboard of the current mainland extent of South China during Permian to Jurassic [*Isozaki et al.*, 2010, 2014; *Cocks and Torsvik*, 2013; *Fujisaki et al.*, 2014] and provided Late Paleozoic and Early Mesozoic detritus for the Yong'an Basin.

5.3. Late Paleozoic to Early Mesozoic Tectonic Setting and Evolution of the South China Craton

Previous models for the tectonic evolution of the South China Craton in Late Paleozoic to Early Mesozoic have debated the relative contributions of convergence along the southern Tethyan margin versus that along the eastern Paleo-Pacific margin of the craton [*Li et al.*, 2012; *Li and Li*, 2007; *Wang et al.*, 2013a; *Yang et al.*, 2012a]. Integration of our data from the Yong'an Basin with data from the contemporaneous Shiwandashan Basin to the southwest and the Youjiang Basin to the west suggests both margins played a role in the evolving tectonic framework in Triassic times whereas the subduction of the Paleo-Pacific played a dominated role in the Permian and Jurassic.

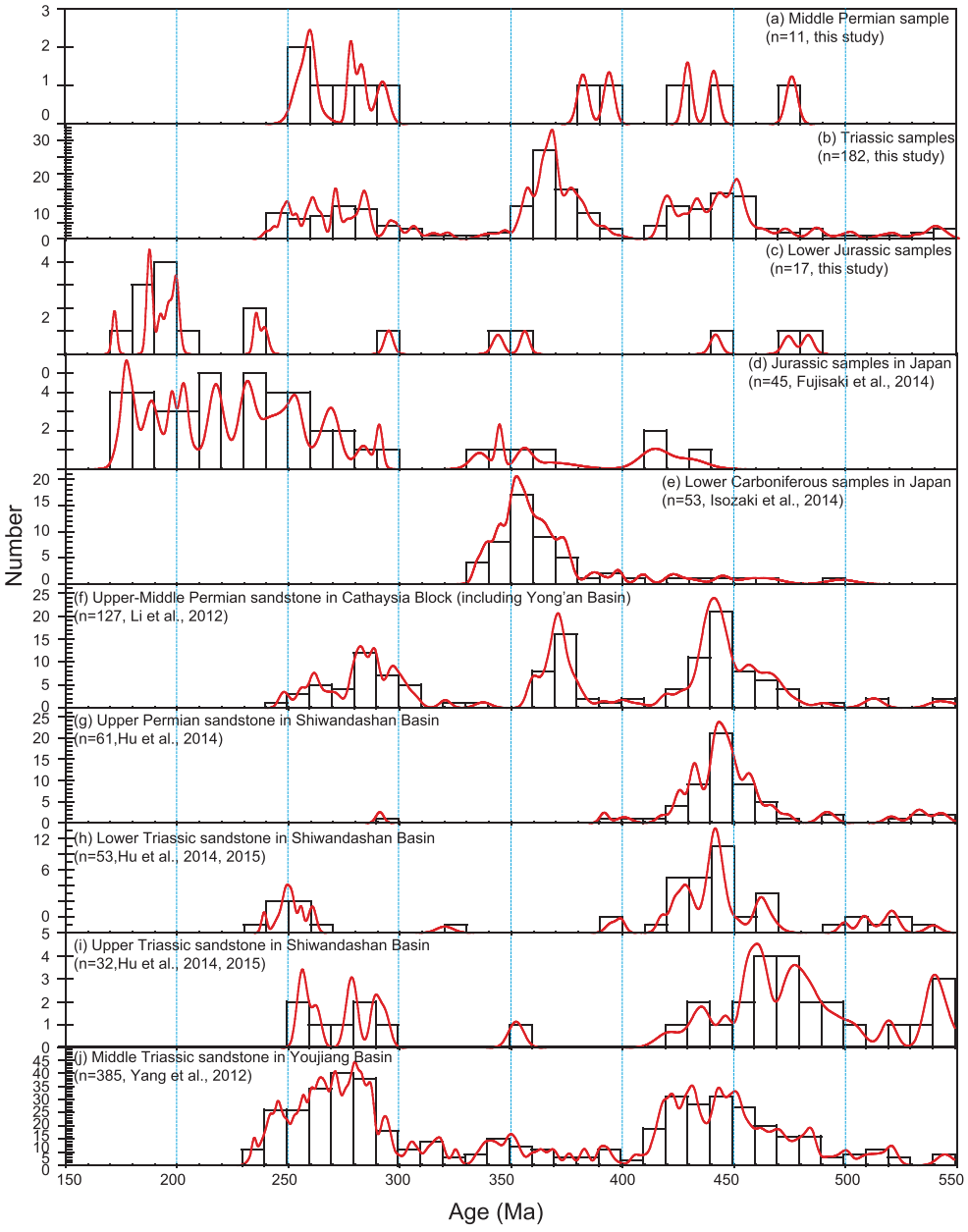

Figure 11. Probability density diagram comparing Phanerozoic detrital zircons models in Permian-Jurassic succession from the Yong'an Basin [this study], Cathaysia Block [*Li et al.*, 2012], Youjiang Basin [*Yang et al.*, 2012a], Shiwandashan Basin [*Hu et al.*, 2014, 2015], and Southwest Japan [*Isozaki et al.*, 2014; *Fujisaki et al.*, 2014].

The provenance history of the Permian to Jurassic sedimentary rocks in the Yong'an Basin suggests accumulation in an evolving retroarc foreland basin. Early Paleozoic and older detritus was derived from the South China Craton inboard of the basin, but younger Paleozoic and Mesozoic detritus is inferred to be derived from magmatic arc sources forming outboard extensions of the craton [*Chen et al.*, 2013; *Herzig et al.*, 1997; *Li et al.*, 2006; *Sakashima et al.*, 2003; *Tagiri et al.*, 2011] (Figure 9). Limited paleocurrent and facies distribution data support multidirection source regions [*Li et al.*, 1997] (Figures 2 and 3). Petrographic and modal data indicate an evolving input from inboard and outboard sources. Middle Permian and Early Triassic to early Middle Triassic rocks in the Yong'an Basin were dominated by quartz grains (70%–90%) with relatively minor feldspar and lithic fragments, indicating significant input from the craton interior. Lithic detritus, including volcanic fragments, increase through the Middle Permian to Early

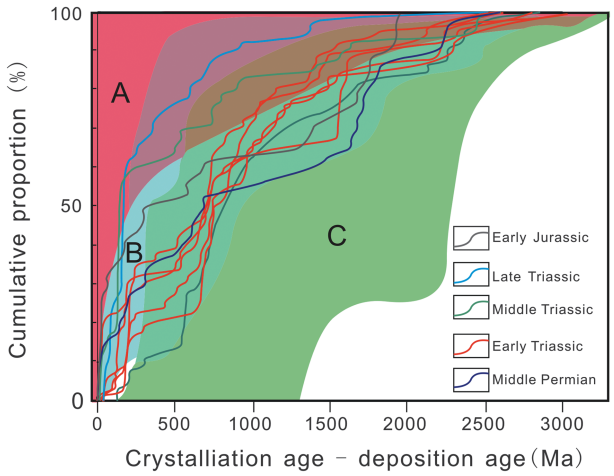

Figure 12. Cumulative probability curves of measured crystallization age for a detrital zircon grains relative to the depositional age of Permian-Jurassic rock samples in the Yong'an Basin (modified from *Cawood et al.* [2012]). Convergent basin (A, rose red), collisional basin (B, blue), and extensional basin (C, green), transition between convergent-collisional setting (purple), convergent-extensional setting (brown), and collisional-extensional setting (blue - green and brown).

Triassic and from the Middle Triassic to Early Jurassic, indicating a greater input from the outboard magmatic arc source. Figure 12 is a cumulative probability plot displaying the difference between the measured crystallization age of detrital zircon grains and the depositional age of the succession in which they occur. All Permian-Jurassic samples from the Yong'an Basin lie in the synorogenic field falling between the convergent and extensional basin fields. Middle Triassic to Lower Jurassic samples are displaced toward the transition zone between convergent and synorogenic basin fields [*Cawood et al.*, 2012]. This data are consistent with our proposed back-arc (retroarc) foreland basin setting in which detritus is a mixture of material from both the craton (extensional source) and the magmatic arc (convergent source) (Figure 13).

Ordovician-Silurian (460–420 Ma) and Late Permian-Triassic (260–230 Ma) orogenic events in the South China Craton resulted in widespread coeval metamorphic and magmatic rocks [*Wang et al.*, 2013a] (Figure 9), and these events are recorded in the detritus supplied to the Permo-Triassic samples in the Yong'an, Shiwandashan, and Youjiang basins of the South China Craton (Figures 10 and 11). Late Devonian to Early Carboniferous (400–340 Ma) and Early to Middle Permian (300–260 Ma) detrital zircons age groups are also present in the Permo-Triassic samples of the Yong'an Basin (Figures 7, 10, and 11). Sedimentary facies relations for the Yong'an Basin in Middle Permian to Early Jurassic along with available paleocurrent data in the Early Triassic succession [*Li et al.*, 1997] (Figures 2 and 3) limit potential source areas of these young grains to Japan and Hainan Islands. Late Cambrian granite and metamorphic rock [*Ding et al.*, 2002], Carboniferous magmatic and metamorphic rocks [*Chen et al.*, 2013; *Ding et al.*, 2005], and Permian granitic rocks [*Li et al.*, 2006, 2002a, 2002b; *Xie et al.*, 2006] (Figure 9) are present in the Hainan Island and in part correspond to the Carboniferous-Permian Renge, Akiyoshi, Maizuru, Ultra-Tamba, and Kurosegawa belts in Japan [*Herzig et al.*, 1997; *Sakashima et al.*, 2003; *Tsujimori and Itaya*, 1999]. Thus, we proposed Hainan Island represents a preserved fragment of a more extensive outboard belt that lay along the Paleo-Pacific Ocean margin of South China in Late Paleozoic to Early Mesozoic. Although Middle Paleozoic (400–340 Ma) rocks form only a minor reported component of the South China Craton [*Zhao et al.*, 2013], detrital zircons of this age are abundant in Permo-Triassic clastic rocks in southeast China [*Li et al.*, 2012, and this study], supporting the possibility of this Late Devonian to Early Carboniferous event.

The Shiwandashan, Youjiang, and Yong'an basins record a history of basin inversion involving shallowing from marine carbonate to terrestrial deposits. This occurred in the early Permian in the Yong'an Basin, the Late Permian in the Shiwandashan Basin, and in the middle Triassic in the Youjiang Basin [e.g., *Hu et al.*, 2014, 2015; *Liang and Li*, 2005; *Yang et al.*, 2012a, 2013; *Zu et al.*, 2012]. Paleocurrents data and detrital zircon age patterns for coeval Permian and Triassic strata in the three basins indicate significant differences in provenance history (Figures 10, 11, and 13). Middle Triassic strata in the Youjiang Basin are mainly derived from the Jinshajiang-Ailaoshan suture zone and the pre-Permian rocks in the Cathaysia Block (Figures 2 and 13), whereas the Shiwandashan Basin contains detritus from the Yunkai Massif and collision-related rock units along the southern margin of the craton related to closure of the Paleo-Tethys Ocean in Permian-Triassic [*Hu et al.*, 2014, 2015; *Liang and Li*, 2005; *Yang et al.*, 2012a, 2013] (Figure 13). Early Paleozoic and Precambrian detrital zircon grains are a minor component of the Middle to Upper Triassic succession in the Yong'an Basin but more common in contemporaneous strata in the Shiwandashan and Youjiang basins (Figure 10).

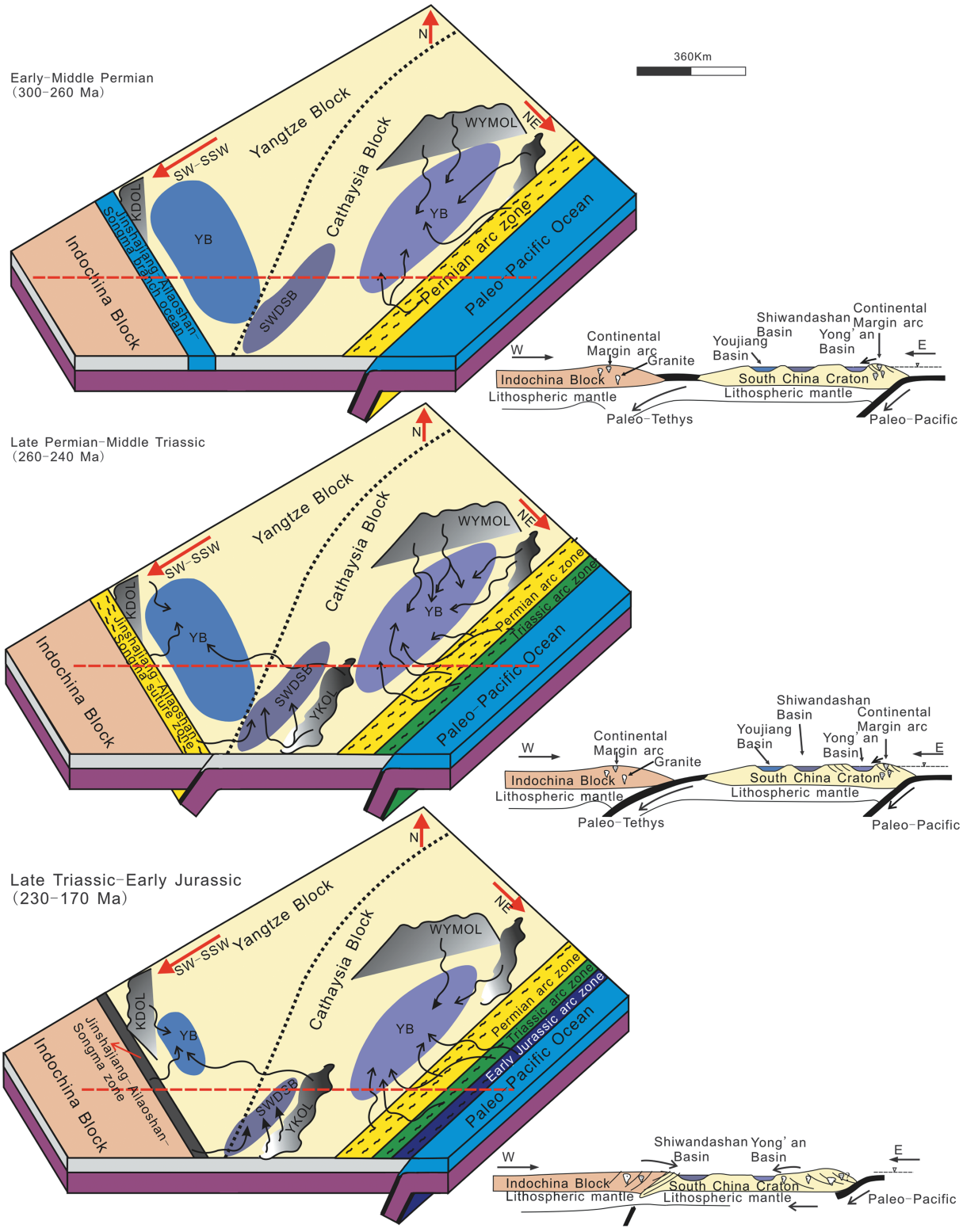

Figure 13. Model for schematic paleogeographic evolution of the South China Craton during the Permian to Jurassic, showing derivation of detritus in the Yong'an Basin from Wuyi Mountain and accretionary orogenic complex in the southeast of the basin; Permian-Jurassic sedimentary basins in the southern margin of the craton record different provenance history indicating that both the Paleo-Tethys and Paleo-Pacific realms were affecting craton evolution in Late Paleozoic to Early Mesozoic. Data for the Youjiang and Shiwandashan basins are from *Yang et al.* [2012a, 2013] and *Hu et al.* [2014, 2015]; subduction of the Paleo-Tethys and Paleo-Pacific ocean are modified from *Zi et al.* [2013], *Li and Li* [2007], and *Isozaki et al.* [2010]. Abbreviation: KDOL, Kangdian Old Land; YB, Youjiang Basin; SWDSB, Shiwandashan Basin; YB, Yong'an Basin; WYMOL, Wuyi Mountain region (Cathaysia old land); YKOL, Yunkai Old land (Yunkai Massif).

The evolution of the differences between the Shiwandashan, Youjiang, and Yong'an basins reflect their position within the South China Craton and the influence of subduction of the Paleo-Tethys beneath the southwestern margin of the craton and the Paleo-Pacific beneath the southeastern margin. The Permian-Jurassic strata in the Yong'an Basin are considered to be derived from a southeastern accretionary orogenic source related to the subduction of the Paleo-Pacific plate [*Cocks and Torsvik*, 2013; *Isozaki et al*., 2010] and from the basement units in the Wuyi Mountain region and correlatives [this study] (Figure 13). The geologic record for the southwestern margin of the South China Craton included subduction of the Paleo-Tethys in the Permian to Early Triassic followed by collision with Indochina in Early to Middle Triassic [*Jian et al*., 2009a, 2009b; *Zi et al*., 2013, and references therein; *Faure et al*., 2014] (Figure 13). The unconformity at the base of the Upper Triassic strata in the Yong'an Basin could reflect the effect of this orogenic event. The Shiwandashan Basin occupied a foreland basin setting in the Late Permian, which was related to Late Permian to Early Triassic collision to the south [*Liang and Li*, 2005; *Roger et al*., 2012; *Zhao et al*., 2012]. This event predates the late Early to Middle Triassic Youjiang foreland basin, the formation of which is related to the timing of ocean basin closure and mountain building in the vicinity of the Jinshajiang-Ailaoshan suture zones [*Jian et al*., 2009a, 2009b; *Yang et al*., 2012a; *Zi et al*., 2013]. The timing for closure of the Paleo-Tethys and subsequence collision of outboard blocks onto the south Asia margin is inferred to have been diachronous, decreasing from southeast to northwest [*Hu et al*., 2015]. Subduction of the Paleo-Pacific in the Permian along southeastern margin of the craton might be the inducement for the diachronous closure of Paleo-Tethys and oblique collision of outboard blocks. Following closure of the Paleo-Tethys, the Late Triassic to Early Jurassic history of the South China Craton was dominated by the Paleo-Pacific domain [*Zhou et al*., 2006] with the Yong'an Basin occupying a retroarc foreland basin position to the Late Triassic to Early Jurassic offshore magmatic arc.

6. Conclusions

Model analysis, detrital zircon U-Pb and trace element data from Permian to Jurassic sandstones of the Yong'an Basin, located along the southeastern coast of the South China Craton indicate a diverse and mixed provenance. Pre-Middle Paleozoic sources lay inboard of the basin whereas Middle Paleozoic to Early Mesozoic sources lay at and outboard of the South China mainland.

Precambrian (circa 3500–500 Ma) and Early Paleozoic (circa 460–420 Ma) zircon groups in the Permian-Jurassic samples overlap with the age of Paleoproterozoic basement, Neoproterozoic igneous, metamorphic, and metasedimentary rock units, and Early Paleozoic granitic rocks in the Wuyi Mountain region and the Yunkai Massif exposed within the South China Craton to the north and southwest of the basin. Late Devonian to Early Carboniferous (circa 400–340 Ma) and Early to Middle Permian (circa 300–260 Ma) detrital zircon groups are mainly derived from rocks exposed along the southeastern margin of the craton or from rocks beyond the coastline and now exposed on Hainan Island and Japan and constituting part of a contemporaneous orogenic system related to subduction of the Paleo-Pacific. This source region has been fragmented and destroyed by subsequent strike-slip activity and tectonic erosion [*Isozaki et al*., 2010, 2014; *Uno et al*., 2011]. The Yong'an Basin occupying a retroarc foreland basin between these various source terranes.

Time equivalent sedimentary basins (Permo-Triassic) to the Yong'an Basin that lie to the southwest and west, the Shiwandashan and Youjiang basins [*Hu et al*., 2014, 2015; *Yang et al*., 2012a], record input from sources situated along the southern margin of the craton and related to subduction and closure of the Paleo-Tethys Ocean.

Integration of our data from the Yong'an Basin with data from the contemporaneous Shiwandashan and Youjiang basins suggests a record the continuous subduction of the Paleo-Pacific Ocean along southeast margin of the South China Craton and termination of subduction of the Paleo-Tethys beneath its southwest margin in Permo-Triassic. Subduction of the Paleo-Pacific along the southern margin of the South China Craton in the Permian might be linked to the final subduction and closure of the Paleo-Tethys beneath the southwest margin of the craton, which displays a record of diachronous closure of the Paleo-Tethys from southeast to southwest and oblique collision of the outboard blocks in the south Asia.

Acknowledgments
The data for this paper are available as Data Sets S1–S3. Figures S1 and S2 are in the supporting information Text S1. This work was supported by the National Natural Science Foundation of China (41272120) and "111 project" (grant B08030), the fundamental Research Funds for the Central Universities, China University of Geosciences (Wuhan). The first author thanks the China Scholarship Council (201406410010). We thank Yongsheng Liu, Zhaochu Hu, and Shu Zheng for their help with zircon LA-ICP-MS U-Pb dating. Detailed comments from two anonymous reviewers led to significant improvements in the manuscript.

References

Bureau of Geology and Mineral Resources of Fujian Province (BGMRFP) (1985), *Regional Geology of Fujian Province* [in Chinese with English abstract], Geol. Publ. House, Beijing.
Bureau of Geology and Mineral Resources of Guangxi Zhuang Autonomous Region (1985), *Regional Geology of Guangxi Zhuang Autonomous Region* [in Chinese with English abstract], Geol. Publ. House, Beijing.
Bureau of Geology and Mineral Resources of Guizhou Province (1987), *Regional Geology of Guizhou* [in Chinese with English abstract], Geol. Publ. House, Beijing.
Bureau of Geology and Mineral Resources of Guangdong Province (1988), *Regional Geology of Guangdong Province* [in Chinese with English abstract], Geol. Publ. House, Beijing.
Bureau of Geology and Mineral Resources of Hunan Province (BGMRHN) (1988), *Regional Geology of Hunan Province* [in Chinese with English abstract], Geol. Publ. House, Beijing.
Bureau of Geology and Mineral Resources of Sichuan Province (1991), *Regional Geology of Sichuan Province* [in Chinese With English Abstract], Bur. of Geol. and Miner. Resour. of Sichuan Province, Geol. Publ. House, Beijing.
Cai, J. X., and K. J. Zhang (2009), A new model for the Indochina and South China collision during the Late Permian to the Middle Triassic, *Tectonophysics*, *467*(1–4), 35–43.
Carter, A., D. Roques, C. Bristow, and P. Kinny (2001), Understanding Mesozoic accretion in Southeast Asia: significance of Triassic thermotectonism (Indosinian orogeny) in Vietnam, *Geology*, *29*(3), 211–214.
Cawood, P., and A. Nemchin (2000), Provenance record of a rift basin: U/Pb ages of detrital zircons from the Perth Basin, Western Australia, *Sediment. Geol.*, *134*(3), 209–234.
Cawood, P. A. (1983), Modal composition and detrital clinopyroxene geochemistry of lithic sandstones from the New England Fold Belt (east Australia): A Paleozoic forearc terrane, *Geol. Soc. Am. Bull.*, *94*(10), 1199–1214.
Cawood, P. A., A. A. Nemchin, M. Freeman, and K. Sircombe (2003), Linking source and sedimentary basin: Detrital zircon record of sediment flux along a modern river system and implications for provenance studies, *Earth Planet. Sci. Lett.*, *210*(1), 259–268.
Cawood, P. A., A. Kröner, W. J. Collins, T. M. Kusky, W. D. Mooney, and B. F. Windley (2009), Accretionary orogens through Earth history, *Geol. Soc. London Spec. Publ.*, *318*(1), 1–36.
Cawood, P. A., C. Hawkesworth, and B. Dhuime (2012), Detrital zircon record and tectonic setting, *Geology*, *40*(10), 875–878.
Cawood, P. A., Y. Wang, Y. Xu, and G. Zhao (2013), Locating South China in Rodinia and Gondwana: A fragment of greater India lithosphere?, *Geology*, *41*, 903–906.
Chang, E. Z. (1996), Collisional orogen between north and south China and its eastern extension in the Korean Peninsula, *J. Southeast Asian Earth Sci.*, *13*(3), 267–277.
Chen, X. Y., Y. J. Wang, M. Wei, W. M. Fan, and T. P. Peng (2006), Microstructural characteristics of the NW-Trending shear zones of Gongai region in Hainan Island and its 40Ar-39Ar geochronological constraints [in Chinese with English abstract], *Geotecton. Metallog.*, *30*(3), 312–319.
Chen, X. Y., Y. J. Wang, W. M. Fan, F. F. Zhang, T. P. Peng, and Y. Z. Zhang (2011), Zircon La-ICP-MS U-Pb dating of granitic gneisses from Wuzhishan area Hainan, and geological signficances [in Chinese with English abstract], *Geochemica*, *40*(5), 454–463.
Chen, X. Y., Y. J. Wang, Y. Z. Zhang, F. F. Zhang, and S. N. Wen (2013), Geochemical and geochronological characteristics and its tectonic significance of Andesitic Volcanic Rocks in Chenxing Area, Hainan [in Chinese with English abstract], *Geotecton. Metallog.*, *37*(1), 99–108.
Cocks, L. R. M., and T. Torsvik (2013), The dynamic evolution of the Palaeozoic geography of eastern Asia, *Earth Sci. Rev.*, *117*, 40–79.
Compston, W., I. Williams, J. Kirschvink, Z. Zichao, and M. Guogan (1992), Zircon U-Pb ages for the Early Cambrian time-scale, *J. Geol. Soc.*, *149*(2), 171–184.
Dickinson, W. R. (1985), Interpreting provenance relations from detrital modes of sandstones, in *Provenance of Arenites*, pp. 333–361, D. Reidel, Dordrecht, Netherlands.
Dickinson, W. R., and C. A. Suczek (1979), Plate tectonics and sandstone compositions, *Am. Assoc. Pet. Geol. Bull.*, *63*(12), 2164–2182.
Dickinson, W. R., and R. Valloni (1980), Plate settings and provenance of sands in modern ocean basins, *Geology*, *8*(2), 82–86.
Dickinson, W. R., et al. (1983), Provenance of North American Phanerozoic sandstones in relation to tectonic setting, *Bull. Geol. Soc. Am.*, *94*(2), 222–235.
Ding, S., C. Xu, W. Long, Z. Zhou, and Z. Liao (2002), Tectonic attribute and geochronology of meta-volcanic rocks Tunchang, Hainan Island [in Chinese with English abstract], *Acta Petrol. Sin.*, *18*(1), 83–90.
Ding, S., J. Hu, B. Song, M. Chen, S. Xie, and Y. Fan (2005), U-Pb dating of zircon from the bed parallel anatectic granitic intrusion in the Baoban group in Hainan Island and the tectonic implication, *Sci. Chin. Ser. D: Earth Sci.*, *48*(12), 2092–2103.
Faure, M., C. Lepvrier, V. V. Nguyen, V. T. Vu, W. Lin, and Z. C. Chen (2014), The South China block-Indochina collision: Where, when, and how?, *J. Asian Earth Sci.*, *79*, 260–274.
Fujii, M., Y. Hayasaka, and K. Terada (2008), SHRIMP zircon and EPMA monazite dating of granitic rocks from the Maizuru terrane, southwest Japan: Correlation with East Asian Paleozoic terranes and geological implications, *Isl. Arc*, *17*(3), 322–341.
Fujisaki, W., Y. Isozaki, K. Maki, S. Sakata, T. Hirata, and S. Maruyama (2014), Age spectra of detrital zircon of the Jurassic clastic rocks of the Mino-Tanba AC belt in SW Japan: Constraints to the provenance of the mid-Mesozoic trench in East Asia, *J. Asian Earth Sci.*, *88*, 62–73.
Gao, S., W. Ling, Y. Qiu, Z. Lian, G. Hartmann, and K. Simon (1999), Contrasting geochemical and Sm-Nd isotopic compositions of Archean metasediments from the Kongling high-grade terrain of the Yangtze craton: Evidence for cratonic evolution and redistribution of REE during crustal anatexis, *Geochim. Cosmochim. Acta*, *63*(13), 2071–2088.
Herzig, C. T., D. L. Kimbrough, and Y. Hayasaka (1997), Early Permian zircon uranium-lead ages for plagiogranites in the Yakuno ophiolite, Asago district, Southwest Japan, *Isl. Arc*, *6*(4), 396–403.
Horie, K., M. Yamashita, Y. Hayasaka, Y. Katoh, Y. Tsutsumi, A. Katsube, H. Hidaka, H. Kim, and M. Cho (2010), Eoarchean–Paleoproterozoic zircon inheritance in Japanese Permo-Triassic granites (Unazuki area, Hida Metamorphic Complex): Unearthing more old crust and identifying source terranes, *Precambrian Res.*, *183*(1), 145–157.
Hoskin, P. W. O., and T. R. Ireland (2000), Rare earth element chemistry of zircon and its use as a provenance indicator, *Geology*, *28*(7), 627–630.
Hoskin, P. W. O., and U. Schaltegger (2003), The composition of zircon and igneous and metamorphic petrogenesis, *Rev. Mineral. Geochem.*, *53*(1), 27–62.
Hu, L., Y. Du, P. A. Cawood, Y. Xu, W. Yu, Y. Zhu, and J. Yang (2014), Drivers for late Paleozoic to early Mesozoic orogenesis in South China: Constraints from the sedimentary record, *Tectonophysics*, *618*, 107–120.
Hu, L., P. A. Cawood, Y. S. Du, Y. J. Xu, W. C. Xu, and H. W. Huang (2015), Detrital records for Upper Permian-Lower Triassic succession in the Shiwandashan Basin, South China and implication for Permo-Triassic (Indosinian) orogeny, *J. Asian Earth Sci.*, *98*, 152–166.

Hu, X., Z. Huang, J. Wang, J. Yu, K. Xu, L. Jansa, and W. Hu (2011), Geology of the Fuding inlier in southeastern China: Implication for late Paleozoic Cathaysian paleogeography, *Gondwana Res.*, *22*, 507–518.
Igi, S., H. Hattori, and K. Shibata (1979), Nomo metagabbro complex and their 450 m.y. ages as a clue to the basement geology—A proposal of 'Saihi Structural Zone' including the pre-Silurian basements in the westernmost part of the Japanese Islands [in Japanese with English abstract], in *The Basement of the Japanese Islands*, edited by H. Kano, pp. 261–280, Tokyo Printing, Sendai.
Ishiga, H. (1990), Paleozoic radiolarians, in *Pre-Cretaceous Terranes of Japan*, edited by K. Ichikawa et al., pp. 285–295, Publication of IGCP-224, Nippon Insatsu Osaka.
Ishiwatari, A., and T. Tsujimori (2003), Paleozoic ophiolites and blueschists in Japan and Russian Primorye in the tectonic framework of East Asia: A synthesis, *Isl. Arc*, *12*(2), 190–206.
Isozaki, Y. (1996), Anatomy and genesis of a subduction-related orogen: A new view of geotectonic subdivision and evolution of the Japanese Islands, *Isl. Arc*, *5*(3), 289–320.
Isozaki, Y., and S. Maruyama (1991), Studies on orogeny based on plate tectonics in Japan and new geotectonic subdivision of the Japanese Islands [in Japanese with English abstract], *J. Geogr.*, *100*, 697–761.
Isozaki, Y., K. Aoki, T. Nakama, and S. Yanai (2010), New insight into a subduction-related orogen: A reappraisal of the geotectonic framework and evolution of the Japanese Islands, *Gondwana Res.*, *18*(1), 82–105.
Isozaki, Y., K. Aoki, S. Sakata, and T. Hirata (2014), The eastern extension of Paleozoic South China in NE Japan evidenced by detrital zircon, *GFF*, *136*(1), 116–119.
Jian, P., D. Liu, A. Kröner, Q. Zhang, Y. Wang, X. Sun, and W. Zhang (2009a), Devonian to Permian plate tectonic cycle of the Paleo-Tethys Orogen in southwest China (II): Insights from zircon ages of ophiolites, arc/back-arc assemblages and within-plate igneous rocks and generation of the Emeishan CFB province, *Lithos*, *113*(3), 767–784.
Jian, P., D. Liu, A. Kröner, Q. Zhang, Y. Wang, X. Sun, and W. Zhang (2009b), Devonian to Permian plate tectonic cycle of the Paleo-Tethys Orogen in southwest China (I): Geochemistry of ophiolites, arc/back-arc assemblages and within-plate igneous rocks, *Lithos*, *113*(3), 748–766.
Kim, S. W., S. Kwon, H. J. Koh, K. Yi, Y.-J. Jeong, and M. Santosh (2011), Geotectonic framework of Permo–Triassic magmatism within the Korean Peninsula, *Gondwana Res.*, *20*(4), 865–889.
Kuwahara, K., A. Yao, and S. Yamakita (1998), Reexamination of Upper Permian radiolarian biostratigraphy [in Japanese with English abstract], *Earth Sci.*, *52*(5), 391–404.
Lepvrier, C., H. Maluski, N. Van Vuong, D. Roques, V. Axente, and C. Rangin (1997), Indosinian NW-trending shear zones within the Truong Son belt (Vietnam) 40Ar-39Ar Triassic ages and Cretaceous to Cenozoic overprints, *Tectonophysics*, *283*(1–4), 105–127.
Lepvrier, C., N. Van Vuong, H. Maluski, P. Truong Thi, and T. Van Vu (2008), Indosinian tectonics in Vietnam, *C. R. Geosci.*, *340*(2–3), 94–111.
Li, P. J., Q. L. Hou, J. L. Li, and S. Sun (1997), Turbidites in the Lower Triassic Xikou Formation in Southwestern Fujian, South China [in Chinese with English abstract], *Acta Sedimentol. Sin.*, *15*(4), 50–57.
Li, S. X., P. Yun, Y. Fan, and J. B. Zhou (2005), Sr and Nd isotopic constraints on the source regions of the Triassic granitoids in central-northern Hainan Island and their significance [in Chinese with English abstract], *Geotecton. Metallog.*, *29*(2), 227–233.
Li, W. X., X. H. Li, and Z. X. Li (2008a), Middle Neoproterozoic syn-rifting volcanic rocks in Guangfeng, South China: Petrogenesis and tectonic significance, *Geol. Mag.*, *145*(4), 475–489.
Li, W. X., X. H. Li, Z. X. Li, and F. S. Lou (2008b), Obduction-type granites within the NE Jiangxi Ophiolite: Implications for the final amalgamation between the Yangtze and Cathaysia Blocks, *Gondwana Res.*, *13*(3), 288–301.
Li, X. (1997), Timing of the Cathaysia Block formation: Constraints from SHRIMP U-Pb zircon geochronology, *Episodes*, *20*(3), 188–192.
Li, X. H., H. Zhou, S. L. Chung, S. Ding, Y. Liu, C. Y. Lee, W. Ge, Y. Zhang, and R. Zhang (2002a), Geochemical and Sm–Nd isotopic characteristics of metabasites from central Hainan Island, South China and their tectonic significance, *Isl. Arc*, *11*(3), 193–205.
Li, X. H., Z. X. Li, W. X. Li, and Y. Wang (2006), Initiation of the Indosinian orogeny in South China: Evidence for a Permian magmatic arc on Hainan Island, *J. Geol.*, *114*(3), 341–353.
Li, X. H., W. X. Li, Z. X. Li, and Y. Liu (2008c), 850-790 Ma bimodal volcanic and intrusive rocks in northern Zhejiang, South China: A major episode of continental rift magmatism during the breakup of Rodinia, *Lithos*, *102*(1–2), 341–357.
Li, X. H., Z. X. Li, B. He, W. X. Li, Q. L. Li, Y. Y. Gao, and X. C. Wang (2012), The Early Permian active continental margin and crustal growth of the Cathaysia Block: In situ U-Pb, Lu-Hf and O isotope analyses of detrital zircons, *Chem. Geol.*, *328*, 195–207.
Li, Z. X., and X. H. Li (2007), Formation of the 1300-km-wide intracontinental orogen and postorogenic magmatic province in Mesozoic South China: A flat-slab subduction model, *Geology*, *35*(2), 179–182.
Li, Z. X., X. Li, H. Zhou, and P. D. Kinny (2002b), Grenvillian continental collision in south China: New SHRIMP U-Pb zircon results and implications for the configuration of Rodinia, *Geology*, *30*(2), 163–166.
Li, Z. X., J. A. Wartho, S. Occhipinti, C. L. Zhang, X. H. Li, J. Wang, and C. Bao (2007), Early history of the eastern Sibao Orogen (South China) during the assembly of Rodinia: New mica 40Ar/39Ar dating and SHRIMP U-Pb detrital zircon provenance constraints, *Precambrian Res.*, *159*(1–2), 79–94.
Li, Z. X., X. H. Li, J. A. Wartho, C. Clark, W. X. Li, C. L. Zhang, and C. Bao (2010), Magmatic and metamorphic events during the early Paleozoic Wuyi-Yunkai orogeny, southeastern South China: New age constraints and pressure-temperature conditions, *Geol. Soc. Am. Bull.*, *122*(5–6), 772–793.
Liang, X., and X. Li (2005), Late Permian to Middle Triassic sedimentary records in Shiwandashan Basin: Implication for the Indosinian Yunkai Orogenic Belt, South China, *Sediment. Geol.*, *177*(3–4), 297–320.
Ling, W., S. Gao, B. Zhang, H. Li, Y. Liu, and J. Cheng (2003), Neoproterozoic tectonic evolution of the northwestern Yangtze craton, South China: Implications for amalgamation and break-up of the Rodinia Supercontinent, *Precambrian Res.*, *122*(1), 111–140.
Liu, R., H. W. Zhou, L. Zhang, Z. Q. Zhong, W. Zeng, H. Xiang, S. Jin, X. Q. Lu, and C. Z. Li (2009), Paleoproterozoic reworking of ancient crust in the Cathaysia Block, South China: Evidence from zircon trace elements, U-Pb and Lu-Hf isotopes, *Chin. Sci. Bull.*, *54*(9), 1543–1554.
Liu, Y., S. Gao, Z. Hu, C. Gao, K. Zong, and D. Wang (2010), Continental and oceanic crust recycling-induced melt–peridotite interactions in the Trans-North China Orogen: U–Pb dating, Hf isotopes and trace elements in zircons from mantle xenoliths, *J. Petrol.*, *51*(1–2), 537–571.
Ludwig, K. R. (2003), Isoplot 3.00, in *A Geochronological Toolkit for Microsoft Excel*, *Spec. Publ.*, vol. 4, pp. 1–70, Berkeley Geochronology Center, Berkeley, Calif.
Ma, Y. S., H. Chen, and G. Wang (2009), *Sequence Stratigraphy and Paleogeography of South China* [in Chinese with English abstract], Science Press, Beijing.
Meng, L., Z. X. Li, H. Chen, X. H. Li, and X. C. Wang (2012), Geochronological and geochemical results from Mesozoic basalts in southern South China Block support the flat-slab subduction model, *Lithos*, *132-133*, 127–140.
Meng, Q.-R., and G.-W. Zhang (1999), Timing of collision of the North and South China blocks: Controversy and reconciliation, *Geology*, *27*(2), 123–126.

Metcalfe, I. (2002), Permian tectonic framework and palaeogeography of SE Asia, *J. Asian Earth Sci.*, *20*(6), 551–566.
Metcalfe, I. (2006), Palaeozoic and Mesozoic tectonic evolution and palaeogeography of East Asian crustal fragments: The Korean Peninsula in context, *Gondwana Res.*, *9*(1), 24–46.
Metcalfe, I. (2011), Palaeozoic–Mesozoic history of SE Asia, *Geol. Soc. London Spec. Publ.*, *355*(1), 7–35.
Metcalfe, I. (2013), Gondwana dispersion and Asian accretion: Tectonic and palaeogeographic evolution of eastern Tethys, *J. Asian Earth Sci.*, *66*, 1–33.
Myrow, P. M., N. C. Hughes, J. W. Goodge, C. M. Fanning, I. S. Williams, S. Peng, O. N. Bhargava, S. K. Parcha, and K. R. Pogue (2010), Extraordinary transport and mixing of sediment across Himalayan central Gondwana during the Cambrian–Ordovician, *Geol. Soc. Am. Bull.*, *122*(9–10), 1660–1670.
Nagy, E. A., H. Maluski, C. Lepvrier, U. Schärer, P. T. Thi, A. Leyreloup, and V. Van Thich (2001), Geodynamic significance of the Kontum Massif in Central Vietnam: Composite 40Ar/39Ar and U-Pb ages from Paleozoic to Triassic, *J. Geol.*, *109*(6), 755–770.
Nakae, S., and T. Kurihara (2011), Direct age determination for an Upper Permian accretionary complex (Kirinai Formation), Kitakami Mountains, Northeast Japan, *Palaeoworld*, *20*(2), 146–157.
Nakano, N., Y. Osanai, N. T. Minh, T. Miyamoto, Y. Hayasaka, and M. Owada (2008), Discovery of high-pressure granulite-facies metamorphism in northern Vietnam: Constraints on the Permo-Triassic Indochinese continental collision tectonics, *C. R. Geosci.*, *340*(2–3), 127–138.
Nam, T. N., Y. Sano, K. Terada, M. Toriumi, P. Van Quynh, and L. T. Dung (2001), First SHRIMP U–Pb zircon dating of granulites from the Kontum massif (Vietnam) and tectonothermal implications, *J. Asian Earth Sci.*, *19*(1), 77–84.
Nutman, A. P., Y. Sano, K. Terada, and H. Hidaka (2006), 743 ± 17 Ma granite clast from Jurassic conglomerate, Kamiaso, Mino Terrane, Japan: The case for South China Craton provenance (Korean Gyeonggi Block?), *J. Asian Earth Sci.*, *26*(1), 99–104.
Osanai, Y., N. Nakano, M. Owada, T. N. Nam, T. Toyoshima, T. Tsunogae, and P. Binh (2004), Permo-Triassic ultrahigh-temperature metamorphism in the Kontum massif, central Vietnam, *J. Mineral. Petrol. Sci.*, *99*(4), 225–241.
Osanai, Y., M. Owada, A. Kamei, T. Hamamoto, H. Kagami, T. Toyoshima, N. Nakano, and T. N. Nam (2006), The Higo metamorphic complex in Kyushu, Japan as the fragment of Permo–Triassic metamorphic complexes in East Asia, *Gondwana Res.*, *9*(1), 152–166.
Qiu, Y. M., S. Gao, N. J. McNaughton, D. I. Groves, and W. Ling (2000), First evidence of $>$ 3.2 Ga continental crust in the Yangtze craton of south China and its implications for Archean crustal evolution and Phanerozoic tectonics, *Geology*, *28*(1), 11–14.
Roger, F., H. Maluski, C. Lepvrier, V. T. Van, and J. L. Paquette (2012), LA-ICPMS zircons U/Pb dating of Permo-Triassic and Cretaceous magmatisms in Northern Vietnam–Geodynamical implications, *J. Asian Earth Sci.*, *48*, 72–82.
Sakashima, T., K. Terada, T. Takeshita, and Y. Sano (2003), Large-scale displacement along the Median Tectonic Line, Japan: Evidence from SHRIMP zircon U–Pb dating of granites and gneisses from the South Kitakami and paleo-Ryoke belts, *J. Asian Earth Sci.*, *21*(9), 1019–1039.
Sano, S. (1992), Neodymium isotopic compositions of Silurian Yakumo metagabbros [in Japanese with English abstract], *J. Mineral. Petrologu Econ. Geol.*, *87*, 272–282.
Sano, Y., H. Hidaka, K. Terada, H. Shimizu, and M. Suzuki (2000), Ion microprobe U-Pb zircon geochronology of the Hida gneiss: Finding of the oldest minerals in Japan, *Geochem. J.-Jpn*, *34*(2), 135–154.
Shi, G. R. (2006), The marine Permian of East and Northeast Asia: An overview of biostratigraphy, palaeobiogeography and palaeogeographical implications, *J. Asian Earth Sci.*, *26*(3), 175–206.
Shu, L., M. Faure, B. Wang, X. Zhou, and B. Song (2008), Late Palaeozoic-Early Mesozoic geological features of south China: Response to the Indosinian collision events in southeast Asia, *C. R. Geosci.*, *340*(2–3), 151–165.
Sinclair, H. (1997), Tectonostratigraphic model for underfilled peripheral foreland basins: An Alpine perspective, *Bull. Geol. Soc. Am.*, *109*(3), 324–346.
Sugamori, Y. (2011), Late Permian radiolarians from the Ajima Formation of the Ultra-Tamba Terrane in the Sasayama area, southwest Japan, *Palaeoworld*, *20*(2), 158–165.
Sun, S. S., and W. McDonough (1989), Chemical and isotopic systematics of oceanic basalts: implications for mantle composition and processes, *Geol. Soc. London Spec. Publ.*, *42*(1), 313–345.
Tagiri, M., D. J. Dunkley, T. Adachi, Y. Hiroi, and C. Fanning (2011), SHRIMP dating of magmatism in the Hitachi metamorphic terrane, Abukuma Belt, Japan: Evidence for a Cambrian volcanic arc, *Isl. Arc*, *20*(2), 259–279.
Takahashi, Y., D.-L. Cho, and W.-S. Kee (2010), Timing of mylonitization in the Funatsu Shear Zone within Hida Belt of southwest Japan: Implications for correlation with the shear zones around the Ogcheon Belt in the Korean Peninsula, *Gondwana Res.*, *17*(1), 102–115.
Takayuki, U., K. Makoto, G. Chitaro, and H. Hironobu (2008), Phengite 40Ar/39Ar age of garnet-bearing pelitic schist pelitic schist pebble obtained from conglomerate in the Nedamo Terrane, Northeast Japan, *J. Geol. Soc. Jpn*, *114*, 314–373.
Tang, L. M., H. L. Chen, W. C. Dong, S. F. Yang, Z. Y. Shen, X. G. Chen, and L. L. Fu (2013), Middle Triassic post-orogenic extension on Hainan Island: Chronology and geochemistry constraints of bimodal intrusive rocks, *Sci. China Earth Sci.*, *56*, 789–793.
Tran, T. H., T. A. Tran, T. P. Ngo, T. D. Pham, V. A. Tran, A. E. Izokh, A. S. Borisenko, C. Y. Lan, S. L. Chung, and C. H. Lo (2008), Permo-Triassic intermediate–felsic magmatism of the Truong Son belt, eastern margin of Indochina, *C. R. Geosci.*, *340*(2), 112–126.
Tsujimori, T., and T. Itaya (1999), Blueschist-facies metamorphism during Paleozoic orogeny in southwestern Japan: Phengite K–Ar ages of blueschist-facies tectonic blocks in a serpentinite melange beneath early Paleozoic Oeyama ophiolite, *Isl. Arc*, *8*(2), 190–205.
Tsujimori, T., J. Liou, W. Ernst, and T. Itaya (2006), Triassic paragonite-and garnet-bearing epidote-amphibolite from the Hida Mountains, Japan, *Gondwana Res.*, *9*(1), 167–175.
Tsutsumi, Y., K. Yokoyama, R. Miyawaki, S. Matsubara, K. Terada, and H. Hidaka (2010), Ages of zircons in jadeitite and jadeite-bearing rocks of Japanese islands, *Bull. Nat. Mus. Nat. Sci. Ser. C*, *36*, 19–30.
Uchino, T., M. Kawamura, C. Gouzu, and H. Hyodo (2008), Phengite 40Ar/39Ar age of garnet-bearing phengite schist pebble obtained from conglomerate in the Nedamo Terrane, Northeast Japan [in Japanese with English abstract], *J. Geol. Soc. Jpn*, *113*, 314–317.
Uno, K., K. Furukawa, and S. Hada (2011), Margin-parallel translation in the western Pacific: Paleomagnetic evidence from an allochthonous terrane in Japan, *Earth Planet. Sci. Lett.*, *303*(1), 153–161.
Wakita, K. (2013), Geology and tectonics of Japanese islands: A review—The key to understanding the geology of Asia, *J. Asian Earth Sci.*, *72*, 75–87.
Wan, Y., D. Liu, M. Xu, J. Zhuang, B. Song, Y. Shi, and L. Du (2007), SHRIMP U-Pb zircon geochronology and geochemistry of metavolcanic and metasedimentary rocks in Northwestern Fujian, Cathaysia block, China: Tectonic implications and the need to redefine lithostratigraphic units, *Gondwana Res.*, *12*(1–2), 166–183.
Wang, H., and X. Mo (1995), An outline of the tectonic evolution of China, *Episodes*, *18*, 6–6.
Wang, Q., J. W. Li, P. Jian, Z. H. Zhao, X. L. Xiong, Z. W. Bao, J. F. Xu, C. F. Li, and J. L. Ma (2005), Alkaline syenites in eastern Cathaysia (South China): Link to Permian-Triassic transtension, *Earth Planet. Sci. Lett.*, *230*(3–4), 339–354.

Wang, Y., W. Fan, F. Guo, T. Peng, and C. Li (2003), Geochemistry of Mesozoic mafic rocks adjacent to the Chenzhou-Linwu fault, South China: Implications for the lithospheric boundary between the Yangtze and Cathaysia blocks, *Int. Geol. Rev.*, *45*(3), 263–286.

Wang, Y., F. Zhang, W. Fan, G. Zhang, S. Chen, P. A. Cawood, and A. Zhang (2010), Tectonic setting of the South China Block in the early Paleozoic: Resolving intracontinental and ocean closure models from detrital zircon U-Pb geochronology, *Tectonics*, *29*, TC6020, doi:10.1029/2010TC002750.

Wang, Y., W. Fan, G. Zhang, and Y. Zhang (2013a), Phanerozoic tectonics of the South China Block: Key observations and controversies, *Gondwana Res.*, *23*(4), 1273–1305.

Wang, Y., A. Zhang, P. A. Cawood, W. Fan, J. Xu, G. Zhang, and Y. Zhang (2013b), Geochronological, geochemical and Nd-Hf-Os isotopic fingerprinting of an early Neoproterozoic arc-back-arc system in South China and its accretionary assembly along the margin of Rodinia, *Precambrian Res.*, *231*, 343–371.

Wang, Y.-J., and Q. Yang (2011), Biostratigraphy, phylogeny and paleobiogeography of Carboniferous–Permian radiolarians in South China, *Palaeoworld*, *20*(2), 134–145.

Wang, Y.-J., Q. Yang, Y.-N. Cheng, and J.-X. Li (2006), Lopingian (Upper Permian) radiolarian biostratigraphy of South China, *Palaeoworld*, *15*(1), 31–53.

Wu, Y.-B., Y.-F. Zheng, S. Gao, W.-F. Jiao, and Y.-S. Liu (2008), Zircon U–Pb age and trace element evidence for Paleoproterozoic granulite-facies metamorphism and Archean crustal rocks in the Dabie Orogen, *Lithos*, *101*(3), 308–322.

Wu, Y.-B., J. M. Hanchar, S. Gao, P. J. Sylvester, M. Tubrett, H.-N. Qiu, J. R. Wijbrans, F. M. Brouwer, S.-H. Yang, and Q.-J. Yang (2009), Age and nature of eclogites in the Huwan shear zone, and the multi-stage evolution of the Qinling-Dabie-Sulu orogen, central China, *Earth Planet. Sci. Lett.*, *277*(3), 345–354.

Xia, Y., X.-S. Xu, and K.-Y. Zhu (2012), Paleoproterozoic S-and A-type granites in southwestern Zhejiang: Magmatism, metamorphism and implications for the crustal evolution of the Cathaysia basement, *Precambrian Res.*, *216*, 177–207.

Xiang, H., L. Zhang, H. W. Zhou, Z. Q. Zhong, W. Zeng, R. Liu, and S. Jin (2008), U-Pb zircon geochronology and Hf isotope study of metamorphosed basic-ultrabasic rocks from metamorphic basement in southwestern Zhejiang: The response of the Cathaysia Block to Indosinian orogenic event, *Sci. China Ser. D: Earth Sci.*, *51*(6), 788–800.

Xie, C., J. Zhu, S. Ding, Y. Zhang, T. Fu, and Z. Li (2006), Identification of Hercynian shoshonitic intrusive rocks in central Hainan Island and its geotectonic implications, *Chin. Sci. Bull.*, *51*(20), 2507–2519.

Xie, C. F., J. C. Zhu, Z. J. Zhao, S. J. Ding, T. A. Fu, Z. H. Li, Y. M. Zhang, and D. M. Xu (2005), Zircon SHRIMP U-Pb age dating of garnet acmite syenite: Constraints on the Hercynian-Indosinian tectonic evolution of Hainan Island [In Chinese with English Abstract], *Geol. J. China Univ.*, *11*(1), 47–57.

Xu, D. R., B. Xia, N. Bakun-Czubarow, C. Ma, P. C. Li, B. Bachlinski, and G. H. Chen (2006), Metamorphic characteristics of the Chenxing metabasite massif in Tunchang area, Hainan Island, South China and its tectonic implication [in Chinese with English abstract], *Acta Petrol. Sin.*, *022*(12), 2987–3006.

Xu, D. R., B. Xia, P. C. Li, G. H. Chen, C. Ma, and Y. Q. Zhang (2007), Protolith natures and U-Pb sensitive high mass-resolution ion microprobe (SHRIMP) zircon ages of the metabasites in Hainan Island, South China: Implications for geodynamic evolution since the late Precambrian, *Isl. Arc*, *16*(4), 575–597.

Xu, Y., P. A. Cawood, Y. Du, L. Hu, W. Yu, Y. Zhu, and W. Li (2013), Linking south China to northern Australia and India on the margin of Gondwana: Constraints from detrital zircon U-Pb and Hf isotopes in Cambrian strata, *Tectonics*, *32*, 1547–1558, doi:10.1002/tect.20099.

Xu, Y., P. A. Cawood, Y. Du, H. Huang, and X. Wang (2014), Early Paleozoic orogenesis along Gondwana's northern margin constrained by provenance data from South China, *Tectonophysics*, *636*, 40–51.

Yang, J., P. A. Cawood, Y. Du, H. Huang, and L. Hu (2012a), Detrital record of Indosinian mountain building in SW China: Provenance of the Middle Triassic turbidites in the Youjiang Basin, *Tectonophysics*, *574-575*, 105–117.

Yang, J., P. A. Cawood, Y. Du, H. Huang, and P. Tao (2012b), Large Igneous Province and magmatic arc sourced Permian-Triassic volcanogenic sediments in China, *Sediment. Geol.*, *261-262*, 120–131.

Yang, J., P. A. Cawood, Y. Du, H. Huang, and L. Hu (2013), A sedimentary archive of tectonic switching from Emeishan Plume to Indosinian orogenic sources in SW China, *J. Geol. Soc.*, *171*(2), 269–280, doi:10.1144/jgs2012-143.

Yang, Z. Y. (2013), Detrital zircon U-Pb ages and Lu-Hf isotope analysis of Early Mesozoic sedimentary basins in the southern margin of South China Block: New constrains for Indosinian movement and tectonic transformation, China Univ. of Geoscience, Wuhan master thesis, pp. 1–102.

Yao, J., L. Shu, and M. Santosh (2011), Detrital zircon U-Pb geochronology, Hf-isotopes and geochemistry—New clues for the Precambrian crustal evolution of Cathaysia Block, South China, *Gondwana Res.*, *2–3*, 553–567.

Yao, W. H., Z. Li, W. Li, X. Li, and J. Yang (2014), From Rodinia to Gondwanaland: A tale of detrital zircon provenance analyses from the southern Nanhua Basin, South China, *Am. J. Sci.*, *314*, 278–313.

Yao, W. H., Z. Li, W. Li, and X. Li (2015a), Was there a Cambrian ocean in South China? Insight from detrital provenance analyses, *Geol. Mag.*, *152*(1), 184–191.

Yao, W. H., Z. Li, W. Li, L. Su, and J. Yang (2015b), Detrital provenance evolution of the Ediacaran-Silurian Nanhua foreland basin, South China, *Gondwana Res.*, doi:10.1016/j.gr.2014.10.018.

Yu, J., Q. Liu, X. Hu, Q. Wang, and S. Y. O'Reilly (2013), Late Paleozoic magmatism in South China: Oceanic subduction or intracontinental orogeny?, *Chin. Sci. Bull.*, *58*(7), 788–795.

Yu, J. H., L. Wang, S. O'Reilly, W. Griffin, M. Zhang, C. Li, and L. Shu (2009), A Paleoproterozoic orogeny recorded in a long-lived cratonic remnant (Wuyishan terrane), eastern Cathaysia Block, China, *Precambrian Res.*, *174*(3–4), 347–363.

Yu, J. H., S. Y. O'Reilly, L. Wang, W. L. Griffin, M. F. Zhou, M. Zhang, and L. Shu (2010), Components and episodic growth of Precambrian crust in the Cathaysia Block, South China: Evidence from U-Pb ages and Hf isotopes of zircons in Neoproterozoic sediments, *Precambrian Res.*, *181*(1–4), 97–114.

Yu, J.-H., S. Y. O'Reilly, M.-F. Zhou, W. Griffin, and L. Wang (2012), U–Pb geochronology and Hf–Nd isotopic geochemistry of the Badu Complex, Southeastern China: Implications for the Precambrian crustal evolution and paleogeography of the Cathaysia Block, *Precambrian Res.*, *222*, 424–449.

Yuan, H., S. Gao, X. Liu, H. Li, D. Günther, and F. Wu (2004), Accurate U-Pb age and trace element determinations of zircon by laser ablation-inductively coupled plasma-mass spectrometry, *Geostand. Geoanal. Res.*, *28*(3), 353–370.

Zhang, A., Y. Wang, W. Fan, Y. Zhang, and J. Yang (2012), Earliest Neoproterozoic (ca. 1.0 Ga) arc-back-arc-basin nature along the northern Yunkai Domain of the Cathaysia Block: Geochronological and geochemical evidence from the metabasite, *Precambrian Res.*, *220–221*, 217–233.

Zhang, F., Y. Wang, X. Chen, W. Fan, Y. Zhang, G. Zhang, and A. Zhang (2011), Triassic high-strain shear zones in Hainan Island (South China) and their implications on the amalgamation of the Indochina and South China Blocks: Kinematic and 40Ar/39Ar geochronological constraints, *Gondwana Res.*, *19*, 439–460.

Zhang, K.-J. (1997), North and South China collision along the eastern and southern North China margins, *Tectonophysics*, *270*(1–2), 145–156.

Zhao, G., and P. A. Cawood (1999), Tectonothermal evolution of the Mayuan Assemblage in the Cathaysia Block: Implications for Neoproterozoic collision-related assembly of the South China Craton, *Am. J. Sci.*, *299*(4), 309–339.

Zhao, G., and P. A. Cawood (2012), Precambrian geology of China, *Precambrian Res.*, *222–223*, 13–54.

Zhao, K. D., S. Jiang, T. Sun, W. Chen, H. Ling, and P. Chen (2013), Zircon U-Pb dating, trace element and Sr-Nd-Hf isotope geochemistry of Paleozoic granites in the Miao'ershan-Yuechengling batholith, South China: Implication for petrogenesis and tectonic-magmatic evolution, *J. Asian Earth Sci.*, *74*, 244–264.

Zhao, L., F. Guo, W. Fan, C. Li, X. Qin, and H. Li (2012), Origin of the granulite enclaves in Indo-Sinian peraluminous granites, South China and its implication for crustal anatexis, *Lithos*, *150*, 209–226.

Zhou, M. F., X. H. Li, W. X. Li, Y. Liu, and Z. X. Li (2007), SHRIMP zircon U-Pb geochronological and whole-rock geochemical evidence for an early Neoproterozoic Sibaoan magmatic arc along the southeastern margin of the Yangtze Block, *Gondwana Res.*, *12*(1–2), 144–156.

Zhou, X., T. Sun, W. Shen, L. Shu, and Y. Niu (2006), Petrogenesis of Mesozoic granitoids and volcanic rocks in South China: A response to tectonic evolution, *Episodes*, *29*(1), 26–33.

Zi, J. W., P. A. Cawood, W. M. Fan, Y. J. Wang, E. Tohver, T. C. McCuaig, and T. P. Peng (2012), Triassic collision in the Paleo-Tethys Ocean constrained by volcanic activity in SW China, *Lithos*, *144–145*, 145–160.

Zi, J. W., P. A. Cawood, W. M. Fan, E. Tohver, Y. J. Wang, T. C. McCuaig, and T. P. Peng (2013), Late Permian-Triassic magmatic evolution in the Jinshajiang orogenic belt, SW China and implications for orogenic processes following closure of the Paleo-Tethys, *Am. J. Sci.*, *313*(2), 81–112.

Zu, F. P., L. S. Shu, and C. Li (2012), Evolution features of depositional and tectonic setting from Late Paleozoic to Meso-Cenozoic in the Yong'an Basin [in Chinese with English abstract], *Geol. Rev.*, *58*(1), 126–148.